Genesis of manganese oxide mineralization in the Boleo region and Concepción Peninsula, Baja California Sur: constraints from Pb-Sr isotopes and REE geochemistry

Rafael Del Rio-Salas[1,2,*], Lucas Ochoa-Landín[3], Christopher J. Eastoe[1], Joaquín Ruiz[1], Diana Meza-Figueroa[3], Martín Valencia-Moreno[2], Hugo Zúñiga-Hernández[3], Luis Zúñiga-Hernández[3], Verónica Moreno-Rodríguez[2,4], and Héctor Mendívil-Quijada[2]

[1] Geosciences Department, University of Arizona, 1040 E 4th St, Tucson Arizona, 85721, USA.
[2] Estación Regional del Noroeste, Instituto de Geología, Universidad Nacional Autónoma de México. Colosio y Madrid s/n, 83000, Hermosillo, Sonora, México.
[3] Departamento de Geología, División de Ciencias Exactas y Naturales, Universidad de Sonora, Rosales y Encinas, 83000, Hermosillo, Sonora, México.
[4] Dpto. de Mineralogía y Petrología, Facultad de Ciencias, Universidad de Granada. Avda. Fuentenueva s/n 18002 Granada, España.
** rdelriosalas@gmail.com*

ABSTRACT

Manganese oxide mineralization on the eastern coast of Baja California Sur is intimately related to the Neogene tectonic evolution of the Gulf of California. Manganese is closely associated with the Cu-Co-Zn mineralization of the Boleo district and nearby deposits of Santa Rosalía region and Concepción peninsula. Trace element and rare earth element geochemistry of the manganese oxides provides clear evidence of a hydrothermal origin and excludes the hydrogenous nature for these deposits. Lead isotope data suggest that metal sources for the manganese mineralization along the eastern coast Baja California Sur are mostly the Miocene Andesite of Sierra Santa Lucía volcanics and the Peninsular Ranges batholith rocks. The strontium isotope data indicate that the mineralizing fluids involved in the manganese mineralization from Boleo district resulted from the interaction of two end-members: (1) the Sierra Santa Lucía volcanic rocks and (2) the gypsum member of the Boleo Formation. The geological observations and the available isotope and geochronological data suggest a southward migration of the hydrothermal processes in response to the evolving tectonic context of the opening of the Gulf of California.

Keywords: manganese oxide, mineralization, rare earth elements, Pb-Sr isotopes, Baja California, Mexico.

RESUMEN

La mineralización de óxidos de manganeso de la porción oriental de Baja California Sur está íntimamente relacionada a la evolución tectónica del Golfo de California durante el Neógeno. Estos depósitos de manganeso están a su vez relacionados a la mineralización de Cu-Co-Zn del distrito El Boleo y otros sitios en los alrededores de Santa Rosalía y la Península de Concepción. La geoquímica de elementos traza y elementos de las tierras raras de los óxidos de manganeso muestra claramente un origen hidrotermal y excluye la naturaleza hidrogénica para estos depósitos. Los análisis de isótopos de plomo sugieren que las fuentes del manganeso pudieron haber sido las rocas volcánicas del Mioceno de la

Del Rio-Salas, R., Ochoa-Landín, L., Eastoe, C.J., Ruiz, J., Meza-Figueroa, D., Valencia-Moreno, M., Zúñiga-Hernández, H., Zúñiga-Hernández, L., Moreno-Rodríguez, V., Mendívil-Quijada, H., 2013, Genesis of manganese oxide mineralization in the Boleo region and Concepción Peninsula, Baja California Sur: constraints from Pb-Sr isotopes and REE geochemistry: Revista Mexicana de Ciencias Geológicas, v. 30, núm. 3, p. 482-499.

Sierra Santa Lucía y el batolito Peninsular. Los isótopos de estroncio indican que los fluidos involucrados en la mineralización de manganeso en el distrito El Boleo son el resultado de la interacción entre dos miembros extremos: (1) las rocas volcánicas de Sierra Santa Lucía y (2) el yeso de la Formación Boleo. Las observaciones geológicas y los datos isotópicos y geocronológicos disponibles, sugieren una migración de los procesos hidrotermales hacia el sureste, relacionados al desarrollo del contexto tectónico de la apertura del Golfo de California.

Palabras clave: óxidos de manganeso, mineralización, elementos de las tierras raras, isótopos de Pb-Sr, Baja California, México.

INTRODUCTION

The tectonic evolution of the Gulf of California has produced several isolated basins, magmatism, volcanism, and hydrothermal activity along the gulf (Karig and Jensky, 1972; Atwater, 1989; Hausback, 1984; Sawlan and Smith, 1984; Lonsdale, 1989; Sawlan, 1991; Canet *et al.*, 2005). Different occurrences and metal endowment are present in the Miocene to Pliocene (Au, Ag, Cu, Co, Zn, and Mn) and recent (Au, Ag, Cu, Co, Zn, and Mn) mineral deposits on the eastern coast of Baja California Sur (Wilson and Rocha, 1955; González-Reyna, 1956; Terán-Ortega and Ávalos-Zermeño, 1993; Ochoa Landín *et al.*, 2000; Prol-Ledesma *et al.*, 2004; Conly *et al.*, 2006, 2011; Rodríguez-Díaz *et al.*, 2010). Among these metals, manganese is a key metal in these deposits because its usefulness to constrain metallogenic processes in space and time in the Baja California province.

Manganese oxide mineralization has been classified on the basis of mineralogy and geochemistry to constrain the depositional environments and the origin of the manganese deposits (Bonatti *et al.*, 1972; Crerar *et al.*, 1982; Nicholson, 1992; Roy, 1992). In general, manganese oxides are deposited in a variety of continental and marine environments as a consequence of hydrogenetic, supergene, and hydrothermal processes (Nicholson, 1992; Roy, 1992).

The purpose of this study is to trace the metal sources and examine the geochemistry of the mineralizing fluids involved during the manganese oxide precipitation. In order to elucidate the genesis of the manganese oxide mineralization, the present study uses Pb and Sr isotopic systematics to trace the metal sources involved in the mineralization. Also, the geochemistry of rare earth elements (REE) and other trace elements in the manganese mineralization is employed to characterize the genesis of the manganese mineralization present at the different mineralized mantos in the Boleo district and surroundings areas.

GEOLOGICAL SETTING

The Gulf of California formed as a result of continental rifting and slow transfer of the Baja California Peninsula from North America to the Pacific plate (Lonsdale, 1989; Spencer and Normark, 1989). The Santa Rosalía basin is an incipient rift basin, formed as a result of northwest- to southeast-trending pre-Gulf continental rifting during Late Miocene (Karig and Jensky, 1972; Stock and Hodges, 1989). This basin hosts the Cu-Co-Zn mineralization from the Boleo district as well as the manganese oxide deposits of nearby areas. The Santa Rosalía basin is bounded to the north-northwest by the Pliocene-Quaternary Tres Vírgenes volcanic field and La Reforma caldera, and to the west-southwest by the 24–12 Ma Andesite of Sierra Santa Lucía (ASL) volcanic rocks, and to the east by the Gulf of California (Figure 1).

The oldest rock in the region is a biotite quartz-monzonite dated at 91.2 ± 2.1 Ma (Schmidt, 1975). This intrusive rock corresponds to the southeastern extension of the Mesozoic Peninsular Ranges batholith complex that represents the crystalline basement of Baja California (Gastil *et al.*, 1975). The ASL suite unconformably lies over the biotite quartz-monzonite intrusive. It is more than 1 km thick and mostly consists of andesite, basaltic andesite and basalt flows, tuffs, breccias, agglomerates and tuffaceous sandstones, predominantly of andesitic composition (Sawlan and Smith, 1984). K-Ar geochronology in the ASL volcanic rocks from Santa Rosalía region yielded ages between 24 and 13 Ma (Sawlan and Smith, 1984; Conly *et al.*, 2005). The ASL suite is the result of the oblique subduction of the Farallon-Guadalupe plate under the North American plate along the western margin of Baja California (Atwater, 1989; Londsdale, 1989; Stock and Hodges, 1989). These volcanic rocks are medium-K calc-alkaline and are widely exposed through the Boleo district and the Concepción Peninsula (Sawlan and Smith, 1984). The final stage of the arc volcanism is represented by the Santa Rosalía dacite unit, which consists of lavas, erupted between 13 and 12 Ma (Conly *et al.*, 2005).

Subsequent volcanic activity records the transition from arc to rift volcanism associated with the initial opening of the Gulf of California (Conly, 2003; Conly *et al.*, 2005). The rift-related suite was unconformably emplaced over the ASL volcanic rocks (Figure 2), and consists of three volcanic groups (Conly *et al.*, 2005): 1) the 11–9 Ma lava flows of the Boleo basalts and the basaltic andesites; 2) El

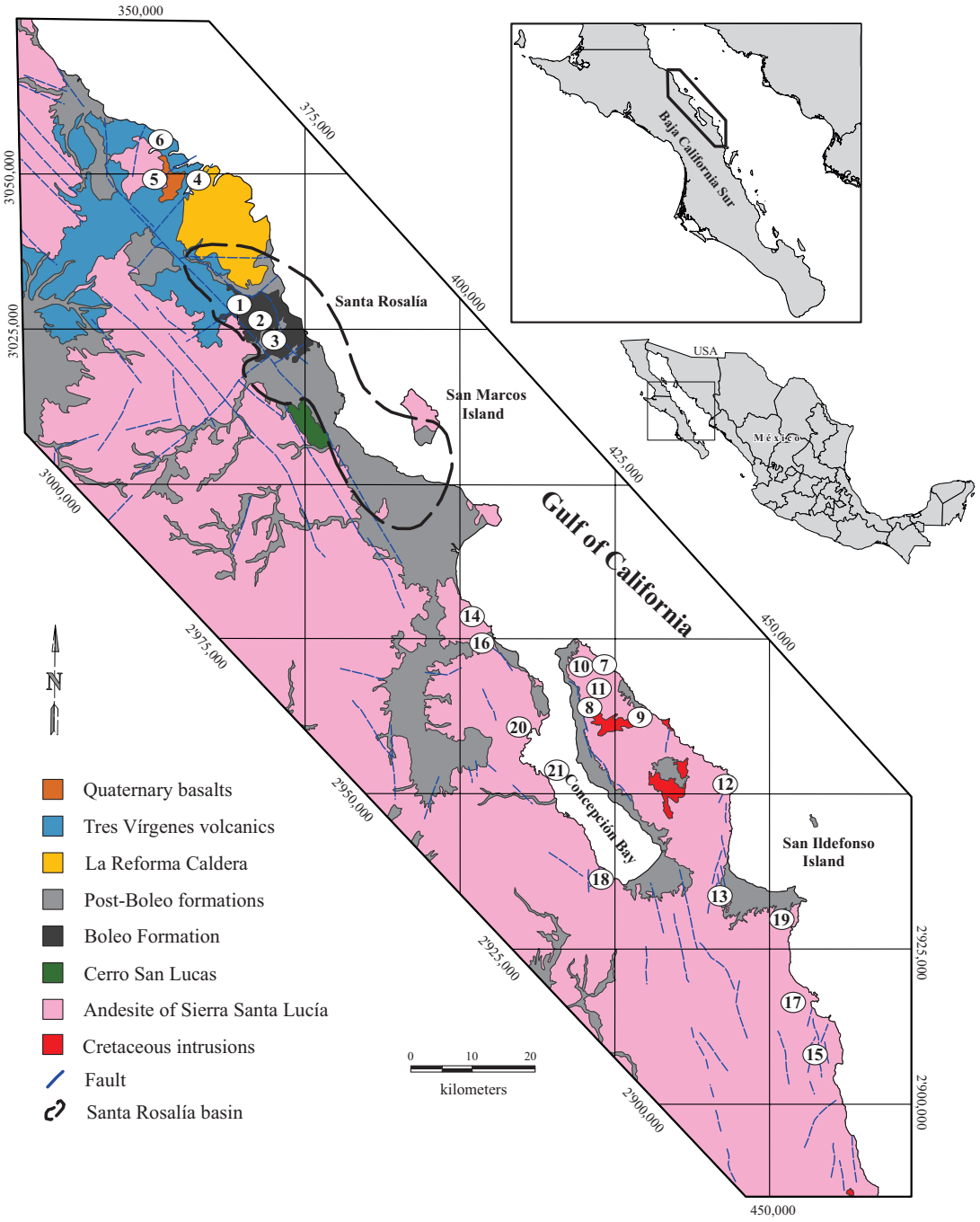

Figure 1. Simplified geological map showing the location of Cu-Co-Zn Boleo district, and other copper and manganese deposits in Baja California Sur, Mexico (modified after Conly *et al.* 2006; Del Rio Salas, 2011). Localities: (1) Lucifer, (2) Neptuno area, (3) Boleo, (4) San Alberto, (5) Rosario, (6) Caracol, (7) Gavilán, (8) Mantitas, (9) La Trinidad, (10) Pilares, (11) Las Minitas, (12) Santa Teresa, (13) Santa Rosa, (14) Las Delicias, (15) Mencenares volcanic field, (16) Mulegé, (17) San Juanico, (18) Azteca, (19) Saquicismunde and Los Volcanes, (20) Santispac, (21) Mapachitos.

Morro tuff, a 9–8 Ma felsic lapilli tuff to ignimbrite unit; and 3) the 9.5 to 7.7 Ma high-K andesitic lava flow of the Cerro San Lucas unit.

The Miocene ASL and rift-related volcanic rocks in the Santa Rosalía region are overlain by a series of sedimentary marine and non-marine formations including the Boleo Formation (Wilson and Rocha, 1955). The thickness of the Boleo Formation varies from 250 to 350 m, and is divided into four members: the basal conglomerate member, the limestone member followed by the gypsum member, and the upper clastic member (Figure 2; Wilson and Rocha, 1955). The basal conglomerate has a maximum thickness of 10 m, and is composed of angular to sub-angular boulders and pebbles derived from the ASL volcanic rocks, supported by a brownish sandy matrix (Wilson and Rocha, 1955); the basal conglomerate is directly overlain by 4 m-thick, red-

dish to brownish, locally fossiliferous, marine limestone (Wilson and Rocha, 1955). The gypsum member overlies either the limestone member or the ASL volcanic rocks, although a rare occurrence is reported where the limestone overlies the gypsum member (Conly, 2003). The gypsum member ranges in thickness from a few meters up to 60 m, and forms massive to distinctly banded beds. The size and shape of these gypsum bodies are variable and range from large horizontal massive beds (hundreds of meters) to small lenses (tens of meters). Overlying the gypsum member is the clastic member, which consists of a series of five coarsening upward fan-delta cycles, with thicknesses ranging between 10 and 140 m (Wilson and Rocha, 1955; Conly, 2003, Conly *et al.*, 2006). However, at least three well-organized cycles are reported (Ochoa-Landín, 1998; Ochoa-Landín *et al.*, 2000), with each cycle ranging between 90 to 100 m in thickness. The clastic cycles consist of siltstones and sandstones at the base, grading upwards to conglomerates (Figure 2). The clastic section has been subdivided into five distinctive lithofacies, which correspond to distinct alluvial fan-delta deposits of a series of progradational episodes. Each deposit was formed in response to a period of basin floor subsidence related to the initial stages of the opening of the Gulf of California (Ochoa-Landín *et al.*, 2000). Holt *et al.* (2000) constrained the age at the base of the Boleo Formation between 7.1 Ma and 6.9 Ma, and from 6.3 to 6.1 Ma at the top. An important stratigraphic marker is present between the sedimentary cycles 3 and 2, which is locally known as "cinta colorada". This unit consists of a thin layer (~0.5 m) of a coarse grained lithic tuff, containing coarse ash to lapilli, mostly andesitic in composition (Wilson and Rocha, 1955). Additionally, pyroclastic volcanism of dacitic to rhyolitic composition is recorded during the deposition of the Boleo Formation, particularly during the deposition of the finest facies (claystone-siltstone) at the beginning of each sedimentary cycle (Ochoa Landín, 1998).

The early to middle Pliocene Gloria Formation (Ortlieb and Colleta, 1984) unconformably lies over the Boleo Formation. The thickness of the Gloria Formation is estimated at ~60 m along the coastal area, and it thins and pinches out inland. The formation grades inland from shallow marine to non-marine conglomerates and sandstones, which locally rest on a basal conglomerate (Wilson and Rocha, 1955). The Gloria Formation is unconformably overlain by the 20–30 m thick Upper Pliocene Infierno Formation (Wilson and Rocha, 1955), which consists of fossiliferous marine sandstone, grading southwest to a continental conglomerate. The Infierno Formation is overlain by the Pleistocene Santa Rosalía Formation (Wilson and Rocha, 1955), which has a thickness of 10–15 m and consists of fossiliferous sandstones and non-marine conglomerates, grading landward to continental breccias and conglomerates (Ortlieb and Colleta, 1984). The most recent lithologies are related to the volcanic activity of Tres Vírgenes, La Reforma caldera, and Mencenares (Camprubí *et al.* 2008; Schmitt *et al.* 2010).

MANGANESE MINERALIZATION IN THE BOLEO REGION

Boleo deposits

The mineralization in the Boleo district consists of laterally extensive and stratiform ore bodies (known as mantos) of disseminated Cu-Co-Zn sulfides and manganese oxides, constrained within the fine-grained facies at the base of each cycle of the Boleo Formation (Figure 2; Wilson and Rocha, 1955; Ochoa-Landín, 1998; Conly, 2003). The mantos are numbered from 4 to 0, with manto 4 being the lowest in the stratigraphic column and manto 0 the uppermost (Wilson and Rocha, 1955).

Manto 4 is commonly related to faults that affected the ASL rocks; these fault zones show evidence of Cu and Mn mineralization (Ochoa-Landín 1998). Manto 4 occurs either above the limestone or the ASL rocks, within the fine-grained facies of the first sedimentary cycle of the Boleo formation, and consists of 1 m-thick laminar calcareous mudstone overlain by a 2 m-thick monomictic breccia with high Mn and Fe oxide content (Wilson and Rocha, 1955). Locally, the Mn and Fe oxides are mixed with jasper that replaced the limestone. The Mn-oxide mineralization in manto 4 occurs directly over the ASL volcanic rocks, and shows dendritic textures within the fine-grained sediments of the Boleo Formation.

Manto 3 is the more extensive and can be continuously traced over an area of 6 × 3 km. The fine-grained facies that host manto 3 consist of a 0.25 to 0.5 m-thick interval of calcareous mudstone at the bottom and a 1 to 20 m-thick fine-laminar claystone-siltstone interval at the top. The later contains a chaotic breccia zone with claystone-siltstone fragments ranging in diameter from 1 to 5 cm, in a claystone-siltstone matrix. The mineralization occurs along the laminar structures of the brecciated fragments and rarely in the matrix (Ochoa-Landín, 1998); however, some authors determined that sulfide mineralization is present in both the fragments and matrix (Bailes *et al.*, 2001; Conly, 2003; Conly *et al.*, 2006; Conly *et al.*, 2011). This manto is important in the district because of its high content of copper minerals, including chalcocite, covellite, chalcopyrite, bornite, native copper, and minor cuprite (Wilson and Rocha, 1955; Ochoa-Landín, 1998). Manganese oxides are present within and above the copper-rich zone, usually as thin horizons along with chrysocolla veinlets, and as small nodules. Locally, the manganese oxide mineralization in manto 3 occurs as nodules, with diameter ranging from 8 to 15 cm, hosted within the fine-grained sediments.

Manto 2 is less extensive, and is also hosted within the fine-grained sediments. The base of the sedimentary sequence consists of a 1 m-thick mudstone, and a 2.5 m-thick breccia zone with siltstone and sandstone fragments in a silty sandstone matrix. The mineralization consists of copper sulfides, mostly chalcocite, along with disseminated pyrite. The manganese content is usually higher at the top

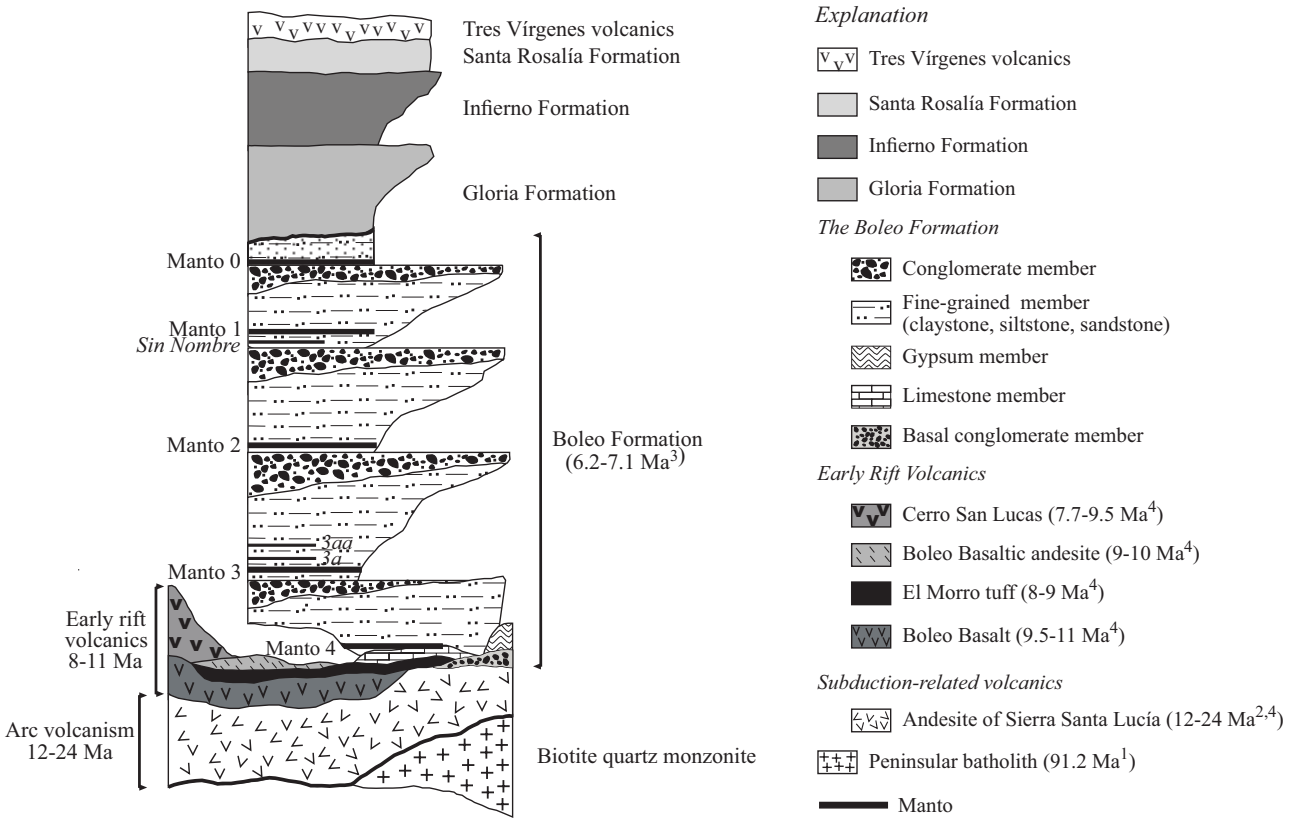

Figure 2. Generalized stratigraphic column of the Santa Rosalía region (modified after Conly *et al.*, 2006; Del Rio Salas *et al.*, 2008). The Cu-Co-Zn mantos and Mn oxide mineralization are located at the beginning of each sedimentary cycle; less important mantos are indicated by italics. Age data from (1) Schmidt (1975); (2) Sawlan and Smith (1984); (3) Holt *et al.* (2000); and (4) Conly (2003).

of the mineralized manto as seen in manto 3. Many of the ores in manto 2 are manganiferous and ferruginous, and are associated with NW-SE silicified structures (Wilson and Rocha, 1955).

A few manganiferous horizons with small quantities of copper are found between mantos 1 and 2, and between mantos 2 and 3. These horizons are commonly discontinuous, thin, and in general, low-grade (Wilson and Rocha, 1955). Manto 1 is the second most important manto after manto 3 as a producer, with ore grade ~4.5% Cu. This manto is the most extensive in the district, but has been productive only in the southeastern portion of the district (Wilson and Rocha, 1955). Manto 0 is the least important of the mantos in the Boleo district. It is commonly manganiferous and ferruginous, and the copper grade is as high as 1% Cu (Wilson and Rocha, 1955).

Neptuno area

The manganese mineralization in Neptuno area correlates with manto 4. It is mostly located near the base of the first sedimentary cycle of the Boleo Formation and is hosted by siltstones and sandstones. These manganese oxide bodies were deposited in lenticular basins (10×15 m) with depths of ~2 m and directly on top of the ASL rocks. These lenticular basins were geomorphic traps that favored the preservation of manganese oxides. In these basins, the Mn and Fe oxides show a strong zonation similar to that observed at the Lucifer deposit. Other manganese oxide outcrops are located directly above the limestone, restricted to N–S fault-controlled depressions. Some manganese oxides with botryoidal morphology are intercalated within the fine-grained sediments below manto 3. In addition to the Mn mineralization in manto 4, the Neptuno area also has evidence of mineralization corresponding to manto 3 just a few meters above manto 4 (Wilson and Rocha, 1955). The mineralization in manto 3 consists of a thin horizon less than 30 cm thick, hosted within claystone-siltstones of the sedimentary cycle 2.

Lucifer deposit

The Lucifer manganese deposit is a stratiform manto deposit hosted within the first sedimentary cycle of the Boleo Formation (manto 4, Figure 2); however, 1 to 5 mm wide manganese oxide veinlets, filling a NW–SE fracture that crosscuts a weakly argillized zone in the ASL rocks has been pointed out by Freiberg (1983). The lower zone of

the Lucifer deposit is composed of a fine-grained sandstone sequence that overlies the limestone member. It contains thin manganese oxides lenses of about 40 cm thickness interbedded within the fine-grained sequence (Freiberg, 1983). These manganese oxide horizons mostly consist of pyrolusite and cryptomelane, and are crosscut by 2 to 5 mm thick silica veins, and are overlain by a 10 m-thick horizon of chaotic breccia, containing angular manganese oxide fragments composed by pyrolusite, cryptomelane, and todorokite. The angular fragments (1 to 5 cm in diameter) represent around 30% of the horizon and are supported in a matrix of Mn oxide. This unit is overlain by a 5 m thick horizon with a brecciated lens composed of angular manganese oxide fragments of similar composition, but with minor content of Fe oxides (hematite and goethite), and jasper fragments, all ranging from 5 to 15 cm in diameter. This lens constitutes the richest manganese ore in the Lucifer deposit, with about 40% Mn. This horizon is overlain by other brecciated lenses, which are massive bodies composed mainly of brecciated jasper. The jasper bodies contain Fe oxides such as goethite and hematite, and are overlain by a breccia with jasper fragments and minor Mn oxide fragments, both ranging from 5 to 20 cm in diameter, supported by a manganese oxide and jasper matrix. The distal facies of the main Mn orebodies in the Lucifer deposit have minor manganese mineralization within fine-grained sediments. The incipient Mn mineralization consists of thin manganese oxide horizons (10–15 cm thick), associated with clay that shows load structures caused by the boulders and pebbles of the conglomerate member.

MANGANESE MINERALIZATION IN THE CONCEPCIÓN PENINSULA

Several localities with manganese oxide mineralization occur along the Concepción Peninsula to the southern part of the Mencenares volcanic field (Figure 1). The manganese mineralization is hosted by volcanic and volcanoclastic rocks, and is constrained by NW-SE fault systems, similarly as in the Santa Rosalía region.

The Gavilán deposit is located at the northeastern tip of the Concepción Peninsula, 15 km east of Mulegé (Figure 1). The hosting rocks in Concepción Peninsula are part of the upper Oligocene to middle Miocene Comondú Group (Hausback, 1984). These volcanic rocks essentially belong to the same volcanic episode that formed the ASL rocks (Sawlan and Smith, 1984). Several name discrepancies exist for these Oligocene-Miocene volcanic rocks (Umhoefer *et al.*, 2001, and references therein). In this work, the nomenclature used for the volcanic rocks from the Concepción Peninsula is from Hausback (1984), since some of the formations that host the manganese mineralization are time constrained.

The manganese mineralization is hosted by andesitic-basaltic lavas of the Pilares Formation from the upper Oligocene to middle Miocene Comondú Group (Camprubí *et al.*, 2008), and consists of a series of NW–SE-oriented manganese oxide veins, which crosscut highly fractured volcanic flows of this formation (Wilson and Veytia, 1949; Noble, 1950). Two types of veins can be distinguished: (1) veins with massive or laminated manganese oxides, and (2) laminated veins with dolomite and quartz that might contain minor manganese oxides (Camprubí *et al.*, 2008). These veins are separated between 2 to 3 m (Wilson and Veytia, 1949), and, in most cases, they are 1 to 10 cm thick, although, some can exceed 0.5 m along fault zones. Also, the manganese mineralization occurs as stockwork with veinlets 1–12 cm thick consisting of pyrolusite with minor coronadite and romanechite, along with dolomite, barite, and vanadinite (Camprubí *et al.*, 2008). The manganese oxides also occurs as breccia matrix; the fragments consist of basaltic and basaltic-andesite lavas with an average diameter around 10 cm. The matrix assemblage is composed by coronadite and minor pyrolusite, and dolomite (Camprubí *et al.*, 2008).

Other less important manganese deposits are present along the Concepción Peninsula (Guadalupe, Minitas, Pilares, Trinidad, Santa Teresa, Azteca mine), and most of them share similar geological features. The manganese mineralization mostly consists of pyrolusite and romanechite, and grades between 4 and 42 wt% Mn. It occurs generally in NW-SE veins systems, hosted in volcanic and volcanoclastic rocks from the Comondú Group (Camprubí *et al.*, 2008). Only two manganese deposits (Santa Rosa and San Juanico mines) show slight differences. The mineralization at the Santa Rosa mine, located south of the Concepción Peninsula, occurs along N-S vertical veins hosted in Pliocene alluvial conglomerates, although the mineralization also replaces the matrix of the same conglomerates (Camprubí *et al.*, 2008; Rodríguez-Díaz *et al.*, 2010). The manganese mineralogy consists of botroidal romanechite or coronadite, along with opal and phanerocrystalline barite. San Juanico mine is located south of the Concepción Peninsula near Cerro Mencenares volcanic filed. The mineralization is related to fault zones within the Comondú Group volcanic rocks and Pliocene limestones of the Infierno Formation, and consists of pyrolusite and romanechite, with Fe oxides and quartz (Camprubí *et al.*, 2008).

ANALYTICAL PROCEDURES

Major and trace elements

Manganese oxides were analyzed for major elements (Mn, Cu, Fe) and some trace elements, including the rare earth elements (REE). For the analysis, pure manganese oxide samples were digested using $HClO_4$ at around 100°C for a few hours, and then the solutions were evaporated to dryness. This step was repeated three times in order to ensure total digestion. Subsequently, the samples were treated with

aqua regia overnight, and then the solutions were evaporated to dryness. The last step was repeated once.

Analysis were performed with an Elan DRC-II inductively coupled plasma – mass spectrometer (ICP-MS) system and a Perkin-Elmer inductively coupled plasma – optical emission spectrometer (ICP-OES) model Optima 4200 DV. Results for the Boleo district samples are shown in Tables 1 and 2, along with data for the Neptuno, Lucifer and Gavilán manganese deposits reported by Del Rio Salas *et al.* (2008).

Lead and strontium isotopes

Whole rock powdered samples were digested using Savillex teflon containers in a 5:1 mixture of HF and HNO_3. The samples were evaporated to dryness and treated with $HClO_4$. After evaporation, concentrated HNO_3 was added to the samples and evaporated to dryness. The samples were treated with 8N HCl and evaporated to dryness. Some steps described above were repeated to ensure total digestion of the samples. Powders from micro-drilled manganese ore

Table 1. Major and trace element concentrations in the manganese oxide ores from the Boleo district, Neptuno, Lucifer and Gavilán manganese deposits in Baja California Sur, Mexico. Concentrations are expressed in ppm, otherwise indicated.

Sample	Comment	Cu (wt%)	Co	Zn	Mn (wt%)	Fe (wt%)	Ni	V	As	Pb	Sr	Ba	Cr	Mn/Fe	Co/Zn	Ref.
Boleo district																
BO 3507	Mn-oxide (º)	5.33	4898	3362	1.34	0.28	106	nd	nd	106	na	na	na	4.72	1.46	2
BO 1007	Manto 2	13.42	12479	38847	2.41	1.51	3856	125	50	719	na	na	na	1.60	0.32	2
95-231b	Manto 3A	5.51	17407	11743	2.62	0.89	415	11	604	151	na	na	na	2.95	1.48	2
95-231e	Manto 3	21.73	1705	15833	19.70	2.07	nd	49	nd	73	na	na	na	9.52	0.11	2
BO 0107	Manto 3	0.72	393	2606	0.84	0.58	4	nd	nd	519	na	na	na	1.46	0.15	2
BO 0407	Manto 3	4.19	3218	4800	0.69	0.40	64	11	32	329	na	na	na	1.74	0.67	2
BO 1907	Manto 3	68.17	nd	8091	9.34	3.29	nd	nd	nd	4162	na	na	na	2.84	-	2
BO 2107	Manto 3	14.83	4682	12864	2.09	1.32	nd	651	399	529	na	na	na	1.58	0.36	2
BO 2207	Manto 3	0.03	nd	1735	5.52	0.73	nd	nd	nd	0	na	na	na	7.52	-	2
BO 1507	Manto 4	6.63	1640	10250	8.19	2.00	nd	nd	nd	82	na	na	na	4.11	0.16	2
BO 2907	Manto 4	5.29	699	11561	1.25	0.42	nd	350	78	1516	na	na	na	2.99	0.06	2
RE 9902a	Manto 4	0.19	1608	17025	52.66	3.90	56	207	na	na	2408	7875	6	13.51	0.09	1
RE 10002	Manto 4	8.38	32	3625	41.47	2.02	58	1228	na	na	13700	49750	245	20.48	0.01	1
BH-1	Mn-vein (*)	13.80	nd	nd	8.61	0.01	nd	101	nd	101	na	na	na	856.00	-	2
Average															*0.44*	
Neptuno area																
RE 9702	Manto 4	2.70	36	1580	na	na	34	185	na	na	2640	9140	230	-	0.02	1
RE 9802a	Manto 4	0.23	1608	3875	58.47	1.87	49	nd	na	na	2395	5300	8	31.19	0.41	1
LF-45	Manto 4	0.10	150	500	na	na	10	20	na	40	1190	1475	na	-	0.30	1
LF-46	Manto 4	0.05	195	858	na	na	15	10	na	45	296	331	na	-	0.23	1
LF-47	Manto 4	0.39	562	2030	na	na	15	135	na	3470	900	1345	na	-	0.28	1
Average															*0.25*	
Lucifer deposit																
RE 4102	Manto 4	na	22	78.90	na	na	72	154	na	na	na	na	na	-	0.28	1
RE 4302 (j)	Manto 4	0.20	30	2408	3.72	11.80	9	644	na	na	91	127	nd	0.32	-	1
RE 4402	Manto 4	0.00	226	1440	37.75	6.35	27	639	na	na	2480	5460	nd	5.94	0.16	1
RE 4502a	Manto 4	0.32	359	2480	na	na	32	967	na	na	2530	6060	nd	-	0.14	1
RE 4602	Manto 4	0.00	350	2043	18.76	3.39	20	480	na	na	2378	4550	35	5.53	0.17	1
RE 5102 (j)	Manto 4	na	2975	242	0.67	15.95	1	497	na	na	78	62	nd	0.04	-	1
RE 5302	Manto 4	0.32	345	793	na	na	59	658	na	na	5690	9350	209	-	0.44	1
RE 5402	Manto 4	0.00	463	1735	61.80	0.29	49	790	na	na	4150	3975	19	212.92	0.27	1
RE 5502	Manto 4	0.10	112	464	na	na	39	522	na	na	3230	3870	11	-	0.24	1
LF-24	Manto 4	0.20	404	1140	na	na	5	745	na	2570	4890	9500	na	-	0.35	1
LF-25	Manto 4	0.12	43	1330	na	na	5	550	na	1105	487	1355	na	-	0.00	1
LF-26	Manto 4	0.14	231	1240	na	na	5	590	na	1770	3830	5180	na	-	0.19	1
Average															*0.22*	
Gavilán deposit, Concepción Peninsula														-		
RE 8602	Mn-vein	0.07	6	903	22.27	1.20	19	372	na	na	440	1583	114	18.56	0.01	1

Notes: (na) Not analized; (nd) below detection limit; (-) not calculated; (*) manganese oxide vein within the Andesite of Sierra Santa Lucía (ASL) rocks; (º) Manganese oxide horizon in sediments from the base of Gloria Formation; (j) Jasperoid. Sources (1) Del Rio Salas *et al.* (2008); (2) present study.

samples were extracted using lead-free tungsten-carbide dental drill bit. The powders were digested using the same procedure described above.

Sr and Pb were separated from the resulting solutions using a chromatographic method following the procedure described by Thibodeau *et al.* (2007). Lead isotope analyses were conducted using a GV Instruments multicollector– inductively coupled plasma – mass spectrometer (MC-ICP-MS) according to the methods discussed in Thibodeau *et al.* (2007). Analysis of NBS-981 standard produced the following results $^{206}Pb/^{204}Pb$ = 16.9405 (± 0.0029 2σ), $^{207}Pb/^{204}Pb$ = 15.4963 (± 0.0034 2σ), and $^{208}Pb/^{204}Pb$ = 36.7219 (± 0.0099 2σ).

The strontium solution separates were loaded on tantalum filaments with Ta gel to enhance ionization following the procedure in Chesley *et al.* (2002). The isotopic analyses were performed by negative thermal ionization mass spectrometry (N-TIMS) using a VG 54 mass spectrometer, according to Chesley *et al.* (2002). Analytical uncertainties (2σ) are $^{87}Sr/^{86}Sr$ = 0.0011% or better.

The obtained lead and strontium isotope data for the manganese oxide mineralization in the Boleo, Neptuno, Lucifer, and Gavilán deposits are shown in Table 3.

RESULTS

Major and trace elements in manganese oxides

In general, the manganese concentration in manto 4 is greater than the concentrations in mantos 3 and 2 (1.2 to 52.7 wt%), with an average concentration of 25.9 wt%. However, copper concentrations in the manganese oxides are lower than those of mantos 3 and 2, ranging from 0.2 to 8.4 wt%. Zinc and cobalt concentrations range from 0.4 to 1.7 wt%, and 32 to 1600 ppm, respectively.

The manganese concentrations from manto 3 range from 0.8 to 19.7 wt%. The copper concentrations in the manganese oxides are higher than in the rest of the mantos and range from 0.03 to 68 wt%. The zinc and cobalt concentrations are higher than concentrations in manto 4, and range from 0.2 to 1.6 wt% and 393 to 4600 ppm, respectively. Mantos 3A and 2 show lower manganese concentrations (~2.5 wt%), and exhibit lower copper content (5.5 and 13.4 wt%, respectively), and higher cobalt and zinc concentrations than manto 3 and 4 (Table 1).

The REE abundances, normalized to the North American shale composite (NASC) from Gromet *et al.* (1984), are shown in Figure 3. The shaded area in Figure 3a represents the REE-normalized trend for the manganese oxides from the different mineralized mantos in the Boleo district. The NASC-normalized La/Sm and Gd/Yb ratios (Table 2) are variable, yielding an average of 2.9 and 1.1, respectively. In general the REE spectrum is relatively flat (Figure 3), yielding an average $(La/Yb)_n$ ratio of 2.4 (Table 2), and is characterized by a positive Eu anomaly.

Pb and Sr isotopes

The lead isotope ratios of the manganese mineralization from manto 4 of the Boleo district are $^{206}Pb/^{204}Pb$ = 18.726 to 18.833, $^{207}Pb/^{204}Pb$ = 15.589 to 15.595, and $^{208}Pb/^{204}Pb$ = 38.471 to 38.499. The Pb isotope values for the manganese mineralization from manto 3 are $^{206}Pb/^{204}Pb$ = 18.708 to 18.800, $^{207}Pb/^{204}Pb$ = 15.588 to 15.598, and $^{208}Pb/^{204}Pb$ = 38.452 to 38.511. The lead data in the manganese oxides from manto 3A is $^{206}Pb/^{204}Pb$ = 18.751, $^{207}Pb/^{204}Pb$ = 15.591 to 15.593, $^{208}Pb/^{204}Pb$ = 38.483 to 38.494. A single manganese oxide from manto 2 has $^{206}Pb/^{204}Pb$ = 18.721, $^{207}Pb/^{204}Pb$ = 15.589, $^{208}Pb/^{204}Pb$ = 38.469.

The lead isotope analysis of manganese oxide from the Lucifer deposit yielded $^{206}Pb/^{204}Pb$ = 18.743 to 18.788, $^{207}Pb/^{204}Pb$ = 15.597 to 15.606, $^{208}Pb/^{204}Pb$ = 38.512 to 38.590. A single lead data of the ASL rocks and a manganese oxide vein from the Gavilán deposit have $^{206}Pb/^{204}Pb$ = 18.621, $^{207}Pb/^{204}Pb$ = 15.584, $^{208}Pb/^{204}Pb$ = 38.432, and $^{206}Pb/^{204}Pb$ = 18.612, $^{207}Pb/^{204}Pb$ = 15.579, $^{208}Pb/^{204}Pb$ = 38.421, respectively.

The Sr isotope data for the manganese oxide mineralization from the Boleo district mantos range from 0.7043 to 0.7067. The strontium isotope data for manganese mineralization from Lucifer deposit range from 0.7050 to 0.7052. The single data for the Neptuno and Gavilán deposits are 0.7067 and 0.7052, respectively.

DISCUSSION

Manganese mineralization and hydrothermal activity

In the Boleo district, the NW-SE structures constituted by manganese oxides and copper silicates crosscut the Andesite of Sierra Santa Lucía (ASL) rocks. Manganese oxide mineralization is also related to the NW-SE structures crosscutting the ASL volcanic rocks in the Lucifer area (Del Rio Salas *et al.*, 2008). The NW-SE structures served as conducts for the ascent of the mineralizing fluids that were discharged into the Santa Rosalía basin. The fact that the mineralizing fluids ascended through these structures is inferred by the juxtaposition of high-grade Cu ± Co zones and localized discordant to stratabound zones of pervasive Mn-Fe-Si alteration (Conly *et al.*, 2006).

Equilibration temperatures using the quartz-pyrolusite geothermometer from Zheng (1991) produced a range of temperatures between 18 and 118 ºC for the manganese oxide mineralization in the different Boleo mantos (Conly, 2003; Conly *et al.*, 2006). The mineralogy and geochemical data suggest a conservative mineralization temperature range between 70 and 118 ºC.

Late Cenozoic hydrothermal activity along a 200 km segment of the eastern coast of Baja California Sur is evidenced by a series of mineralized localities (Figure 1). North of Tres Vírgenes volcanic field, evidence of hydro-

Table 2. Rare earth element concentration in ppm for manganese oxides from the Boleo district, Neptuno, Lucifer and Gavilán manganese deposits in Baja California Sur, Mexico. REE ratios, normalized to the North American shale composite, are also included.

Sample	Comment	La	Ce	Pr	Nd	Sm	Eu	Gd	Tb	Dy	Ho	Er	Tm	Yb	Lu	Σ REE	$(La/Sm)_n$	$(Gd/Yb)_n$	$(La/Yb)_n$	Ref.
Boleo district																				
BO 3507	Mn-oxide^{o}	63.4	99.9	10.1	34.5	6.1	3.6	7.9	0.4	6.8	0.6	5.0	0.3	5.0	0.3	243.8	2.0	0.9	1.3	2
BO 1007	Manto 2	16.4	16.5	1.2	11.9	0.9	0.7	1.0	0.1	0.8	0.2	0.5	0.1	0.4	0.1	50.7	3.6	1.5	4.1	2
95-231b	Manto 3A	25.9	75.4	4.9	49.6	1.8	23.3	1.9	0.3	1.8	0.4	1.2	0.2	1.3	0.2	188.2	2.8	0.8	2.0	2
95-231e	Manto 3	35.2	70.4	4.0	35.1	2.6	9.2	3.0	0.4	2.4	0.5	1.8	0.2	1.4	0.3	166.6	2.6	1.2	2.5	2
BO 0107	Manto 3	11.5	26.5	3.2	12.7	2.7	0.4	2.8	0.2	2.3	0.2	0.5	0.1	0.6	0.1	63.6	0.8	2.8	2.1	2
BO 0407	Manto 3	81.4	230.2	15.0	49.7	7.6	7.6	7.8	0.5	7.8	1.7	5.8	0.3	6.4	0.3	422.1	2.1	0.7	1.3	2
BO 1907	Manto 3	9.6	22.9	2.7	11.2	2.0	0.5	2.2	0.3	1.8	0.4	1.1	0.2	1.1	0.2	56.1	0.9	1.2	0.9	2
BO 2107	Manto 3	231.8	302.0	17.0	72.2	9.1	22.0	10.0	0.6	10.1	0.8	8.3	0.4	8.7	0.5	693.4	4.9	0.7	2.7	2
BO 2207	Manto 3	1.2	2.0	0.2	1.3	0.2	0.3	0.2	0.0	0.2	0.0	0.1	0.0	0.1	0.0	5.9	1.3	1.2	1.2	2
BO 1507	Manto 4	104.7	126.4	12.9	44.4	4.7	3.5	5.6	0.9	5.4	1.2	3.6	0.5	3.1	0.5	317.5	4.2	1.0	3.4	2
BO 2907	Manto 4	8.0	9.7	1.1	10.1	0.2	4.0	0.3	0.0	0.2	0.0	0.1	0.0	0.1	0.0	34.0	7.0	1.4	7.5	2
RE 9902a	Manto 4	90.1	113.3	4.2	21.7	4.3	0.1	4.8	0.7	5.6	1.3	4.8	0.5	4.3	0.6	256.1	4.1	0.6	2.1	1
RE 10002	Manto 4	147.1	267.3	6.7	35.0	11.4	nd	6.8	1.1	9.4	1.9	7.1	0.9	7.9	1.0	503.6	2.5	0.5	1.9	1
BH-1	Mn-vein*	0.5	2.9	0.1	1.1	0.1	0.6	0.1	0.0	0.1	0.0	0.1	0.0	0.1	0.0	5.6	1.6	0.4	0.5	2
Average																*214.8*	*2.9*	*1.1*	*2.4*	
Neptuno area																				
LF-45	Manto 4	9.3	12.5	1.9	5.5	1.0	0.6	1.1	0.2	1.0	0.2	0.7	0.1	0.7	0.1	34.9	1.8	0.9	1.3	1
LF-46	Manto 4	424.0	996.0	90.3	285.0	46.1	20.7	36.1	4.4	18.2	2.6	6.4	0.6	3.5	0.4	1934.3	1.8	5.8	12.1	1
LF-47	Manto 4	41.7	122.0	10.1	30.0	5.5	2.6	3.9	0.6	3.5	0.6	1.6	0.3	1.9	0.3	224.6	1.5	1.2	2.2	1
RE 9702	Manto 4	28.9	83.2	6.1	21.2	3.4	8.4	3.1	0.5	3.1	0.6	1.8	0.1	1.6	0.2	162.0	1.6	1.1	1.8	1
RE 9802a	Manto 4	122.3	233.0	13.8	51.8	7.9	3.8	7.6	1.0	7.2	1.4	4.8	0.5	3.8	0.5	459.5	3.0	1.1	3.3	1
Average																*563.1*	*1.9*	*2.0*	*4.1*	
Lucifer deposit																				
LF-24	Manto 4	8.6	10.5	1.3	4.5	0.8	0.2	0.8	0.1	0.5	0.1	0.3	0.1	0.3	0.1	28.2	2.1	1.5	2.9	1
LF-25	Manto 4	2.7	7.0	0.6	2.5	0.5	0.1	0.8	0.1	0.6	0.1	0.4	0.1	0.4	0.1	16.0	1.0	1.1	0.7	1
LF-26	Manto 4	5.1	7.5	0.7	2.5	0.5	0.1	0.6	0.1	0.4	0.1	0.2	0.1	0.2	0.1	18.2	2.0	1.7	2.6	1
LF-27	Manto 4	0.5	1.0	0.2	0.5	0.1	0.1	0.1	0.1	0.1	0.1	0.1	0.1	0.1	0.1	3.2	1.0	0.6	0.5	1
RE 4302	Manto 4	2.0	7.4	0.4	1.9	0.4	0.1	0.6	0.1	0.5	0.1	0.4	nd	0.3	0.1	14.5	0.9	1.1	0.6	1
RE 4402	Manto 4	4.0	8.3	0.5	2.8	1.1	0.2	0.5	0.0	0.4	0.1	0.3	nd	0.2	0.0	18.5	0.7	1.5	2.1	1
RE 4602	Manto 4	20.0	22.7	2.8	12.3	2.3	0.2	2.0	0.3	1.6	0.3	1.0	nd	0.8	0.1	66.5	1.7	1.4	2.5	1
RE 4702	Manto 4	9.7	18.3	3.6	15.0	2.8	0.7	2.4	0.4	2.0	0.4	1.3	0.1	1.2	0.2	57.9	0.7	1.2	0.8	1
RE 4802a	Manto 4	9.2	15.5	0.7	3.6	1.8	nd	0.6	0.1	0.5	0.1	0.4	nd	0.3	0.0	32.8	1.0	1.3	3.4	1
RE 5202	Manto 4	2.7	3.4	0.4	2.1	1.6	nd	0.2	nd	0.2	0.0	0.1	0.1	0.1	nd	11.0	0.3	1.7	3.4	1
RE 5402	Manto 4	1.8	3.7	0.2	1.0	0.7	nd	0.2	0.0	0.1	0.0	0.0	nd	0.1	0.0	7.9	0.5	1.6	2.9	1
RE 5902	Manto 4	8.1	7.1	0.8	4.6	1.8	nd	1.0	0.1	0.9	0.1	0.6	0.0	0.5	0.0	25.7	0.9	1.2	1.7	1
Average																*25.0*	*1.0*	*1.3*	*2.0*	
Gavilán deposit, Concepción Peninsula																				
RE 8602	Mn-vein	9.8	8.1	1.1	5.3	1.5	0.1	1.6	0.2	1.9	0.4	1.4	0.1	1.1	0.1	32.9	1.3	0.8	0.9	1

Notes: (nd) Below detection limit; (*) manganese oxide vein within the Andesite of Sierra Santa Lucía (ASL) rocks; (^{o}) manganese oxide horizon in sediments from the base of the Gloria Fm. Sources (1) Del Rio Salas *et al.*, 2008, (2) present study.

thermal activity is recorded by the copper and manganese mineralization within the ASL rocks in the San Alberto prospect, and copper mineralization at the Caracol alteration zone (Figure 1). South of Boleo district, the hydrothermal activity is mostly represented by manganese deposits such as Mantitas, Gavilán, La Trinidad, Pilares, Las Minitas, Santa Teresa, and Azteca (Bustamante-García, 1999; Camprubí *et al.*, 2008). Fluid inclusion microthermometry on barite samples from the Mn-Ba Santa Rosa deposit, southern Concepción Peninsula, yielded a temperature range between 97 and 160 ºC, with two fluid inclusions population: (1) average T_h = 136.5 ºC and 4.2 wt. % equivalent NaCl, and (2) average T_h = 136 ºC and 11.4 wt. % equivalent NaCl (Rodríguez-Díaz *et al.*, 2010).

The geothermal waters from springs and wells in and around the Tres Vírgenes and La Reforma caldera fields located north of the Boleo district (Figure 1) are characterized by temperatures from 21 to 98 ºC (Portugal *et al.*, 2000). South of the Boleo district, localities such as Saquicismunde and Los Volcanes (Figure l), are current

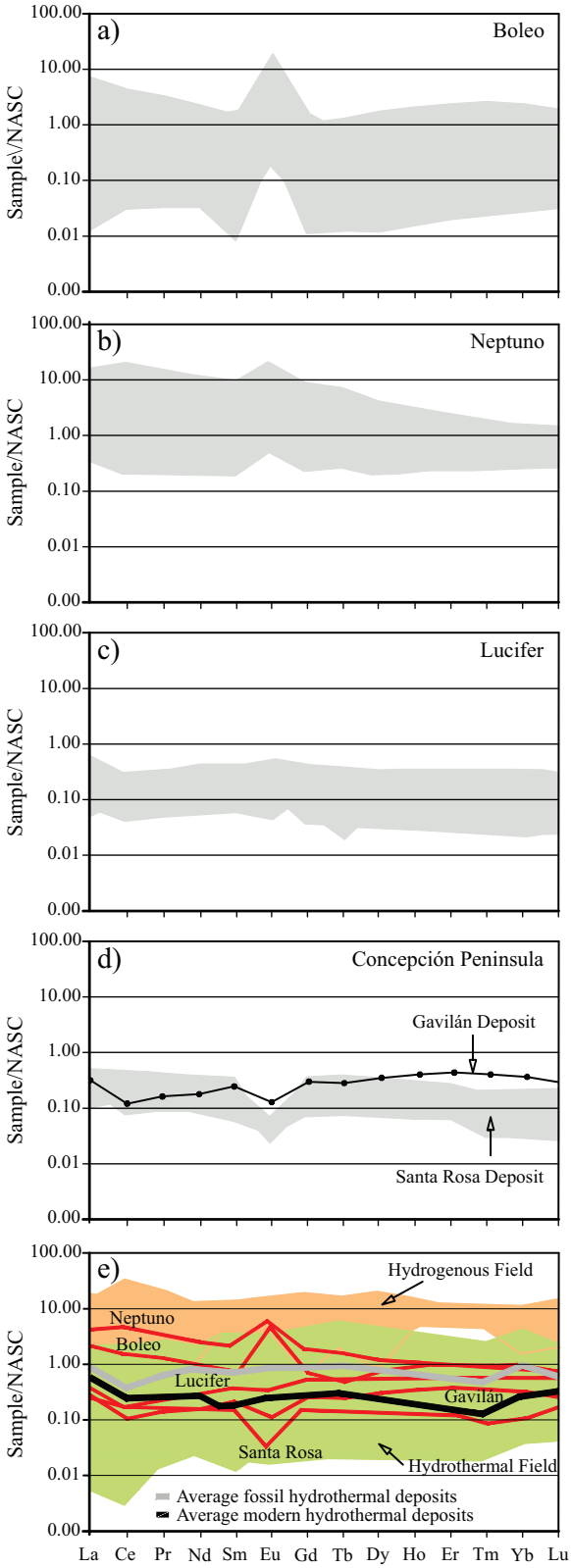

Figure 3. North American shale composite (NASC)-normalized rare earth (REE) element patterns for the manganese oxide mineralization from the Boleo region and the Mn deposits from Concepción Peninsula. REE data for the Mn deposit from Neptuno, Lucifer and the Concepción Peninsula taken from Del Rio Salas *et al.* (2008) and Rodríguez-Díaz *et al.* (2010). REE data for hydrothermal and hydrogenous fields, and average fossil and modern deposits from Usui and Someya (1997).

Table 3. Lead and strontium isotope data of samples from the Boleo district and adjacent deposits in Baja California Sur, Mexico.

Sample	Description	Locality	$^{87}Sr/^{86}Sr$	$^{206}Pb/^{204}Pb$	$^{207}Pb/^{204}Pb$	$^{208}Pb/^{204}Pb$
BO1007	Mn Manto 2	Boleo	-	18.721	15.589	38.469
95-231b	Mn Manto 3A	Boleo	-	18.751	15.593	38.494
95-231b(r)	Mn Manto 3A	Boleo	0.7063	18.751	15.591	38.483
95-231e	Mn Manto 3	Boleo	0.7065	18.720	15.593	38.481
BO0107	Mn Manto 3	Boleo	0.7043	18.727	15.598	38.497
BO0407	Mn Manto 3	Boleo	-	18.762	15.597	38.511
BO1907	Mn Manto 3	Boleo	-	18.708	15.588	38.452
BO2107	Mn Manto 3	Boleo	-	18.740	15.591	38.473
BO2207	Mn Manto 3	Boleo	-	18.800	15.594	38.487
BO0407	Mn Manto 3	Boleo	0.7054	18.758	15.599	38.516
RE9902	Mn Manto 4	Boleo	0.7068	18.731	15.592	38.478
RE10002	Mn Manto 4	Boleo	-	18.833	15.595	38.499
BO1507	Mn Manto 4	Boleo	0.7067	18.726	15.589	38.471
BO2907	Mn Manto 4	Boleo	0.7064	18.742	15.596	38.518
RE9802	Mn Manto 4	Neptuno	0.7067	18.741	15.593	38.493
BO2507	Mn in Gypsum member	Boleo	0.7083	18.719	15.591	38.480
RE4502	Mn Manto 4	Lucifer	0.7052	18.743	15.597	38.512
RE4802	Mn Manto 4	Lucifer	-	18.788	15.606	38.590
RE5402	Mn Manto 4	Lucifer	0.7052	18.759	15.601	38.546
RE5302	Mn Manto 4	Lucifer	0.7050	18.761	15.600	38.546
RE4402	Mn Manto 4	Lucifer	0.7050	18.788	15.604	38.588
RE8602	Mn oxide	Gavilán	0.7052	18.612	15.579	38.421
BH-1	Mn oxide	Boleo	0.7079	18.784	15.594	38.480

Note: (r) repeated sample; (-) not analyzed.

examples of hydrothermal activity that may correspond in type to that responsible for the mineralization in the Boleo district. These geothermal emanations are geographically quite dispersed, and all of them share similar geological features such as the structural northwest-southeast control, the evidence of hydrothermal alteration, the occurrence within the Miocene volcanic or volcanoclastic rocks, and the low temperatures range between 38 to 94 ºC (Casarrubias and Gómez-López, 1994; Bustamante-García, 1999; Camprubí *et al.*, 2008). Hydrothermal activity is also present along the western coast of Concepción Bay, between the Santispac and the Mapachitos areas (Figure l). Temperatures of hydrothermal fluids range between 72 to 87 °C in submarine diffusive venting areas (Canet *et al.*, 2005). Although some of these geothermal emanations occur within the shallow submarine environment (<20 m depth), they share similar features than those exposed above (Prol-Ledesma *et al.*, 2004; Canet *et al.*, 2005).

Mineralization age

The age of the Boleo Formation in the Santa Rosalía region has been previously constrained by Holt *et al.* (2000). The age was calculated using isotope data in conjunction with magnetostratigraphy, which is correlated with the geomagnetic polarity time scale. The most likely correlation

yielded an age of 7.09–6.93 Ma for the base and 6.27– 6.14 Ma for the top of the Boleo Formation (Holt *et al.*, 2000). The manganese mineralization in the Boleo deposit has yielded an age of 7.0 ± 0.2 Ma (Conly *et al.*, 2011), which is stratigraphically and chronologically in agreement with the deposition age for the base of the Boleo Formation. Moreover, the manganese mineralization age is also in agreement with the geochronologic data for the underlying lithologic units in the Santa Rosalía region, which include the 24–13 Ma ASL, the 11–9 Ma Boleo basalts and Boleo basaltic andesites, and the 9–8 Ma El Morro tuff (Conly *et al.*, 2005).

Moreover, the Gulf of California region has been subjected to intense volcanism and tectonic activity (Sawlan 1991). Around the Santa Rosalía region, Conly *et al.* (2005) reported K–Ar ages for the high-K andesites from Cerro San Lucas suite, which represents volcanic activity during the transition from arc- to rift magmatism between 9.5 and 7.7 Ma. Furthermore, Pallares *et al.* (2008) reported geochronologic data supporting the continuation of volcanic activity until the Pleistocene, following the end of the calc-alkaline volcanism northern Santa Rosalía region.

Geochemistry of manganese oxides

Discrimination diagrams for the origin of manganese deposits have been proposed on the basis of the cation-adsorption capacity of manganese oxides, considering the concentrations of specific trace elements present in manganese oxides. These discrimination diagrams have been used to distinguish between a hydrothermal (continental or marine) and a hydrogenous origin. The term hydrothermal refers to manganese oxides deposited directly from geothermal waters around hot springs and pools in continental environments or sedimentary exhalative manganese mineralization deposited in marine environments (Nicholson, 1992 and references therein). The term hydrogenous refers to deposits formed by slow precipitation or adsorption of dissolved components from seawater (Bonatti *et al.*, 1972; Crerar *et al.*, 1982; Nicholson, 1992).

Elements such as Ba, Cu, Ni, Co, Pb, Sr, V, and Zn are frequently found in hydrothermal manganese-rich systems (Nicholson, 1992). These elements are present in significant concentrations in the manganese oxide mineralization from Santa Rosalía region and Concepción Peninsula (Table 1). Hydrothermal oxides have lower Co, Cu, Ni, and Zn concentrations, relative to hydrogenous deposits (Nicholson 1992 and references therein); hence, high cobalt concentrations are indicative of marine environments (hydrogenous). Nicholson (1992) proposed discrimination diagram for hydrothermal and supergene manganese oxide deposits based on the abundance of trace elements (Figure 4); in this diagram the manganese oxides from marine and freshwater environments are included within the supergene field.

Previous studies in Lucifer deposit and the manganese oxides from Concepción Peninsula have documented the hydrothermal nature of the manganese oxide deposits (Canet *et al.*, 2005; Camprubí *et al.*, 2008; Del Rio Salas *et al.*, 2008; Rodríguez-Díaz *et al.*, 2010). In Figure 4, the manganese ore samples reported from Baja California Sur and those from the Boleo mantos plot within the hydrothermal field. In general, the samples from Concepción Peninsula are characterized by lower Co and Ni concentrations, like those from the Lucifer deposit (Figure 4). The data from the Neptuno area plot above the Lucifer and the Concepción Peninsula deposits, and are characterized by higher concentrations of Co and Ni. The Boleo manto samples are relatively richer in Co and Ni compared with the samples mentioned before. Within the Boleo samples, it is possible to notice a relative enrichment from manto 4 to manto 2. The trace element concentrations in the manganese oxides indicate a clear hydrothermal origin for all manganese deposits in the Santa Rosalía region and the Concepción Peninsula.

The shaded area in Figure 3a represents the NASC-normalized REE spectrum for the manganese oxides in the Boleo mantos. No particular difference is observed in the REE enrichment of the different the mantos; the entire spectrum is relatively flat and displays a subtle enrichment of the light rare earth element (LREE) over the heavy rare earth element (HREE), as pointed out with the normalized La/Yb ratios, as well as the noticeable positive Eu anomaly. The normalized REE spectrum of the manganese mineralization from Neptuno area displays also a positive Eu anomaly with relatively flat trends, except for sample LF-46, which is the most enriched in the LREE relative to the NASC, as noticed by the high normalized La/Yb ratio (Table 2) (Del Rio Salas *et al.*, 2008). The REE pattern of the manganese oxides from Lucifer deposit is flat (Figure 3c) as noticed by an average normalized La/Yb ratio of

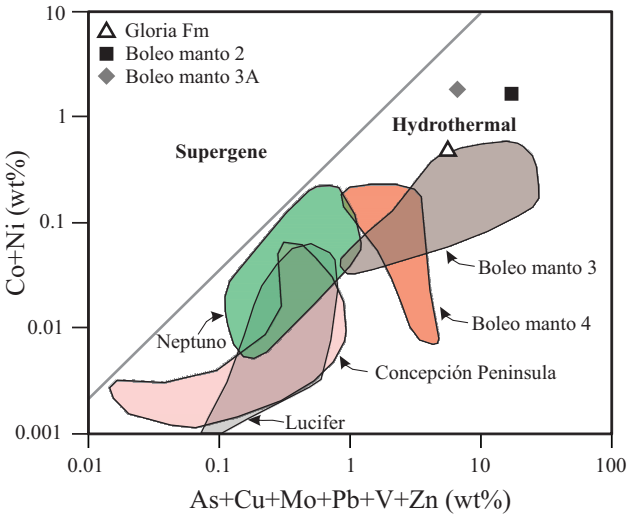

Figure 4. Trace element discrimination diagram for manganese oxides deposits of supergene and hydrothermal origin (Nicholson, 1992). In this diagram the supergene field includes the manganese oxides deposited in fresh water and seawater environments (Nicholson, 1992).

2.0 (Table 2), and they signatures are characterized by the absence of either positive or negative Ce or Eu anomalies (Del Rio Salas *et al.*, 2008).

The available REE data for the manganese oxides from Concepción Peninsula are presented in Figure 3d. A sample from the Gavilán deposit has REE concentrations that are lower than NASC, and a relatively flat REE pattern with an average normalized La/Yb of 0.9, and slightly negative Ce and Eu anomalies (Figure 3d) (Del Rio Salas *et al.*, 2008). Figure 3d also shows the REE data from Santa Rosa manganese oxides, which is depleted in REE with respect to NASC, and has a relatively flat spectrum with slightly Ce and clear Eu negative anomalies (Figure 3d) (Rodríguez-Díaz *et al.*, 2010). In general, the available REE data of the manganese oxides from Concepción Peninsula exhibit relatively flat patterns, characterized by slightly negative Ce and Eu anomalies.

Table 4 shows the average of the total REE abundances of various manganese oxide deposits of hydrothermal and hydrogenous nature. The total REE concentrations in hydrothermal deposits range from 45 to 648 ppm, whereas those for hydrogenous deposits range from 1208 to 1918 ppm (Glasby *et al.*, 1997; Miura and Hariya, 1997; Nath *et al.*, 1992; Nath *et al.*, 1997; Usui and Someya, 1997; Wiltshire *et al.*, 1999). The average of the total REE for the Boleo mantos ranges from 50 to 270 ppm and produce an average of 215 ppm. The average total REE for the manganese oxides from Neptuno area is around 560 ppm; sample LF-46 is characterized by a total REE around 1900 ppm, and excluding this particular sample, the average of total REE is 220 ppm. The average total REE for Lucifer and the deposits in Concepción Peninsula ranges from 25 to 37 ppm.

Figure 3e shows the NASC-normalized REE patterns for manganese oxides from hydrogenous and hydrothermal deposits from Usui and Someya (1997). The pattern for the hydrogenous deposits is enriched relative to the NASC values, whereas the pattern for the hydrothermal deposits is either depleted or slightly enriched than NASC values. This figure also shows the spectrum for the average modern and fossil hydrothermal deposits from Usui and Someya (1997). In addition, this figure includes the average NASC-normalized REE spectra from the manganese deposits from the Boleo and adjacent areas, which are included within the hydrothermal field. The average REE patterns for the Lucifer and Santa Rosa deposits are the most depleted in REE and agree with the average modern hydrothermal deposits. The REE signature of the Gavilán deposit is located between the average modern and average fossil hydrothermal deposits. Finally, the REE signatures for the Boleo and Neptuno deposits are slightly more enriched in REE than the average fossil hydrothermal deposits, but still located within the hydrothermal field (Figure 3e).

In general, NASC-normalized REE patterns for the manganese mineralization around the Boleo district and Concepción Peninsula are relatively flat as noticed from the consistent normalized La/Sm, Gd/Yb, and La/Yb ratios. The REE patterns of the Boleo district and Neptuno area show middle REE enrichment (Figure 3a and 3b), which can be characteristic of hydrogenous manganese samples (Nath *et al.*, 1992, 1997). Also, the REE patterns exhibit very distinctive positive Eu anomalies, which is a characteristic feature of modern hydrothermal deposits in the ocean (Hodkinson *et al.*, 1994), as opposed to the REE signature of seawater, which exhibits a negative Ce anomaly and a slight enrichment of the HREE over the LREE (Douville *et al.*, 1999). Although the mineralization in these deposits is not properly from hydrothermal activity in a marine environment, the Eu enrichment in the manganese ores can be explained by the presence of plagioclase in the fine-grained sediments derived from the ASL rocks. The mobility of Eu depends strongly on redox and temperature conditions (Michard *et al.*, 1983), and Eu enrichment involves hot and reduced fluids, whereas Eu depletion involves cold and oxidizing fluids (Parr, 1992; Canet *et al.*, 2005). Since each manto experienced such redox conditions, a positive Eu anomaly can be explained by the cyclical hydrothermal activity related to the formation of each manto. Moreover, these samples are located within the field of hydrothermal field deposits (Figure 3), and the hydrothermal nature is also confirmed by the total REE in Table 4.

The NASC-normalized REE patterns for the manganese ores from the Lucifer and the manganese deposits from Concepción Peninsula agree with the spectra of the average hydrothermal deposits (Usui and Someya 1997); only the average of total REE for the Gavilán deposit exhibits a subtle enrichment especially in the HREE relative to the average of modern hydrothermal deposits (Figure 3e). Hydrogenous manganese deposits are characterized by a positive Ce anomaly (Fleet, 1983), as a result of the oxidation of Ce^{3+} to Ce^{4+}, which forms highly insoluble CeO_2 in seawater (Elderfield and Greaves, 1981; Fleet, 1983; Nath *et al.*, 1997; Canet *et al.*, 2008). Conversely a negative Ce anomaly is characteristic of hydrothermal Fe-Mn deposits (Fleet, 1983). The slightly negative Eu could be explained by cold and oxidizing fluids (Parr, 1992), as previously reported for the recent Mn mineralization in Concepción Bay (Canet *et al.*, 2005). Furthermore, the total REE content of these deposits confirms their hydrothermal nature when compared to other hydrothermal deposits in Table 4.

In summary, trace element and REE geochemistry in the manganese oxides from the Boleo district and Concepción peninsula, demonstrates the hydrothermal nature of the ores (Figures 3 and 4). The REE enrichments for the Boleo mantos and Neptuno mineralization can be explained by mixing of hydrothermal and hydrogenous sources or by supergene processes.

Metal sources

Lead and strontium isotope data for the Peninsular Ranges batholith and the volcanic rocks in Santa Rosalía

Table 4. Rare earth element average concentrations from hydrothermal and hydrogenous manganese oxide deposits, including those from Baja California.

Locality	La	Ce	Pr	Nd	Sm	Eu	Gd	Tb	Dy	Ho	Er	Tm	Yb	Lu	Σ REE	Ref.
Hydrogenous deposits																
Indian Ocean	153.4	714.1	34.8	142.0	33.8	8.9	43.7	5.7	30.6	5.6	15.5	2.3	15.0	2.2	1207.6	1
Johnston Island	260.0	1201.0	44.8	192.7	35.4	10.1	48.5	6.8	43.7	9.9	28.9	4.3	27.9	3.6	1917.7	2
Pitcairn Island hotspot	276.8	741.7	50.8	214.4	42.7	10.2	49.9	7.2	44.7	9.2	26.4	3.9	26.0	4.0	1508.1	3
Pacific seamounts	202.2	1104.6	106.2	162.4	41.6	9.9	26.0	7.5	57.8	6.6	31.9	4.3	17.7	3.3	1782.0	4
Marginal seamounts	228.2	740.6	51.4	259.4	45.6	10.4	57.0	6.9	46.3	8.9	24.7	3.5	19.4	3.2	1505.4	4
Marginal abyssal plain	228.4	918.4	47.9	220.8	47.5	11.4	53.0	7.3	40.5	7.3	20.2	2.9	17.9	2.8	1626.2	4
Hydrothermal depostis																
Indian Ocean	183.2	163.8	-	164.4	35.3	9.1	37.2	-	34.7	-	-	-	17.6	2.6	647.9	5
Pitcairn Island hotspot	33.8	48.3	9.9	39.1	8.4	2.5	7.5	1.1	6.4	1.1	3.2	0.4	2.6	0.4	164.9	3
Modern hydrothermal	18.9	16.3	-	7.2	1.0	0.3	-	0.3	-	-	-	-	0.8	0.1	44.8	4
Fossil hydrothermal	27.7	25.8	-	24.4	4.2	1.1	-	0.8	-	-	-	-	2.8	0.3	87.1	4
Hokkaido Japan	30.5	140.3	-	43.3	12.6	2.4	-	2.2	-	-	-	-	2.3	1.6	235.0	6
Lucifer deposit	6.2	9.4	1.0	4.4	1.2	0.2	0.8	0.1	0.7	0.1	0.4	0.1	0.4	0.1	25.2	7
Neptuno area	125.2	289.3	24.4	78.7	12.8	7.2	10.3	1.3	6.6	1.1	3.1	0.3	2.3	0.3	563.1	7
Gavilán deposit	9.8	8.1	1.1	5.3	1.5	0.1	1.6	0.2	1.9	0.4	1.4	0.1	1.1	0.1	37.2	7
Santa Rosa	8.5	13.0	1.7	5.5	1.0	0.0	1.0	0.2	0.9	0.2	0.4	0.9	0.3	0.7	34.0	8
Boleo district - all mantos	59.1	97.5	5.9	27.9	3.8	5.8	3.9	0.4	3.9	0.7	2.9	0.3	2.9	0.3	215.2	9
Boleo district - manto 2	16.4	16.5	1.2	11.9	0.9	0.7	1.0	0.1	0.8	0.2	0.5	0.1	0.4	0.1	50.7	9
Boleo district - manto 3A	25.9	75.4	4.9	49.6	1.8	23.3	1.9	0.3	1.8	0.4	1.2	0.2	1.3	0.2	188.2	9
Boleo district - manto 3	61.8	109.0	7.0	30.4	4.0	6.7	4.3	0.3	4.1	0.6	2.9	0.2	3.0	0.2	234.6	9
Boleo district - manto 4	87.5	129.1	6.2	27.8	5.2	2.5	4.4	0.7	5.1	1.1	3.9	0.5	3.8	0.5	278.4	9
Boleo district - Gloria Fm	63.4	99.9	10.1	34.5	6.1	3.6	7.9	0.4	6.8	0.6	5.0	0.3	5.0	0.3	243.8	9

region, the Boleo conglomerate, and the sulfide and manganese oxide mineralization have been reported previously by Conly (2003) and Conly *et al.* (2005, 2006, and 2011). The present study contributes with Pb and Sr isotope data for the lithologic units and the manganese oxide mineralization from the different mantos in the Boleo district as well as for the mineralized zones around the Santa Rosalía region (Table 3). The lead isotope fields for the lithologic units and manganese oxide mineralization are shown in Figure 5 (Conly *et al.*, 2005 and 2011; present study).

Figure 5 shows that the Pb isotope data for the manganese oxide mineralization from the Boleo district reported in the present study are located inside and below the fields for the ASL and Boleo Formation rocks, with the $^{207}Pb/^{204}Pb$ ratios constrained to a limited range between 15.583 and 15.608, and between 38.440 to 38.590 for the $^{208}Pb/^{204}Pb$ ratio, vaguely deviated from the ASL field and at lower Pb-isotope ratios than those of the Peninsular Ranges batholith, which suggests that the principal source of metals in the different mantos in the Boleo district and the manganese mineralization in the Neptuno is mainly the ASL volcanic rocks.

Despite the scarcity of isotopic data for the rift-related rock suite, according to the data for a single sample from the Boleo basalt reported in this study, along with the data for the Cerro San Lucas volcanic rocks, whose $^{206}Pb/^{204}Pb$ ratios range from 18.43 to 18.61 (Conly, 2003), the rift-related suite rocks are characterized by less radiogenic lead, which suggests that the volcanism related to the rifting of the Gulf of California is not contributing to the metal budget in the mineralized areas reported in the present study.

The lead isotope data for the manganese oxides from Lucifer deposit are located within the field of the ASL rocks; however there is a trend towards the Peninsular Ranges batholith member. This suggests that the mineralizing fluids for Lucifer deposit are the result of mixing processes between the ASL and the Peninsular Ranges batholith rocks. This interpretation is supported by field observations along the Arroyo del Infierno in Lucifer area, where the Peninsular Ranges batholith is found underlying the ASL rocks; also, some ASL rocks contain xenoliths of the Peninsular Ranges batholith. In contrast, lead isotope data for the Boleo manganese oxides suggest negligible mixing processes between the ASL and batholith rocks, basically because the ALS rocks act as the basement in the Boleo district.

Lead isotope measurement of a single sample from the Gavilán deposit in Concepción Peninsula, indicate that the ASL rocks in that area are less radiogenic that those from the Santa Rosalía region (Figure 5a), suggesting slight isotopic differences for the sources involved in the genesis of the ASL rocks trend along Baja California (Figure 1). An alternative explanation for the less radiogenic nature of the ASL rocks in the Gavilán deposit is the possibility of the continuation of the regional isotope trend of the ASL rocks from the Boleo district; this is probably reflecting the less radiogenic nature of the underlying rocks along this seg-

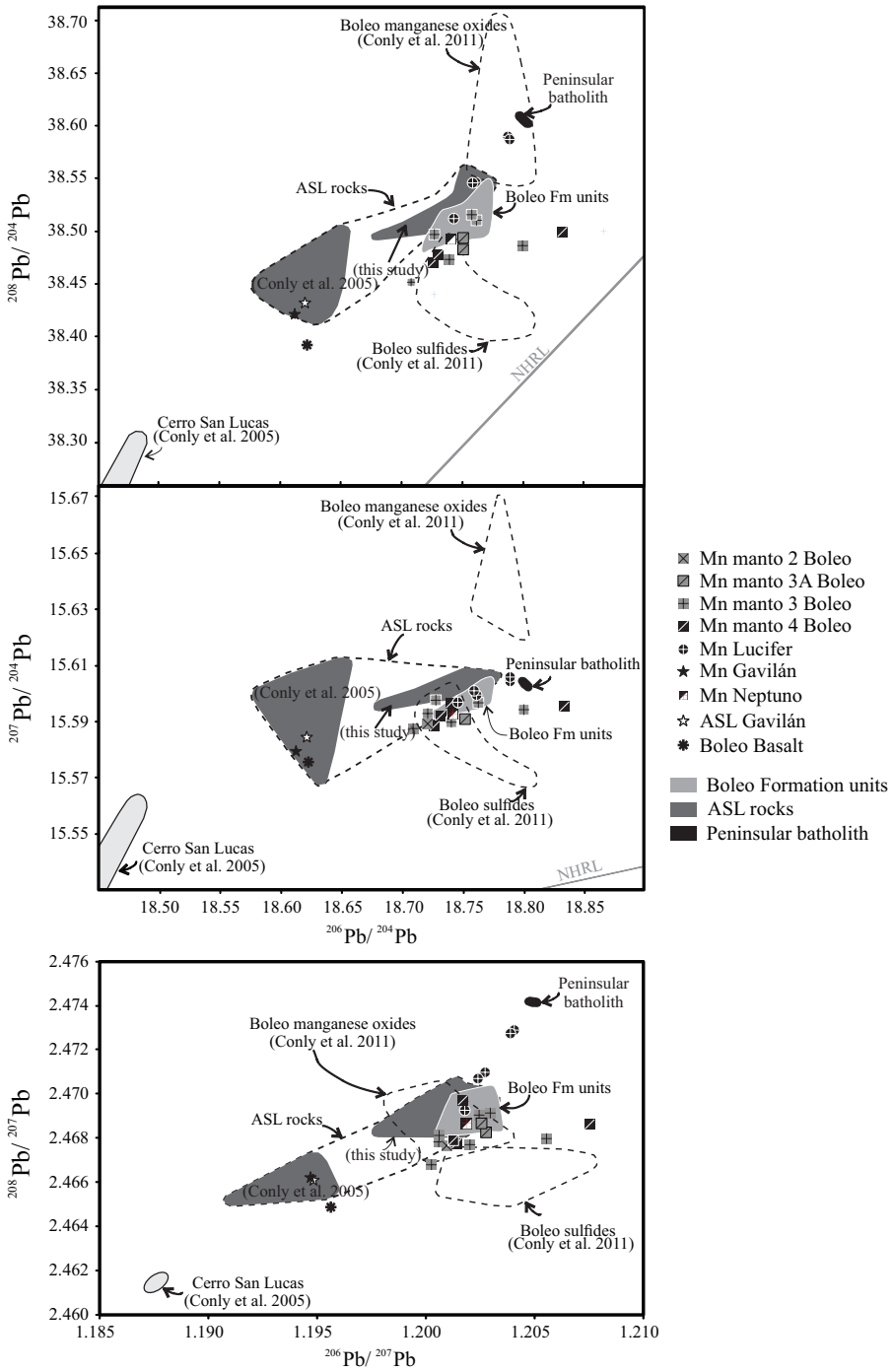

Figure 5. Diagrams showing the lead isotope ratios for the manganese mineralization from the different mineralized mantos and the manganese deposits around Santa Rosalía. ASL: Andesite of Sierra Santa Lucía; NHRL: Northern Hemisphere Reference Line.

ment of the Baja California Peninsula. The manganese oxide sample from the Gavilán deposit exhibits the same isotopic signature as the ASL rocks, suggesting that the source of metals in the mineralized zones is in the ASL rocks.

The similarity of the $^{206}Pb/^{204}Pb$ ratios of the manganese oxides and manto sulfides demonstrate that the fluids responsible for the Cu-Co-Zn mineralization are similar to those that precipitated the Mn oxides of the Boleo district, although significant differences are noted in the $^{208}Pb/^{204}Pb$ and $^{207}Pb/^{204}Pb$ ratios suggesting a more radiogenic lead in the manganese oxides than in the manto sulfides (Conly *et al.* 2011). The slight shift to higher $^{206}Pb/^{207}Pb$ ratios of the Boleo manto sulfides is interpreted as the result of the interaction of Pb from basin seawater with ferromagnesian minerals from the arc-to-rift volcanic rocks and $^{206}Pb/^{207}Pb$-enriched seawater fluids that interacted with the Cretaceous quartz-monzonite basement (Conly *et al.* 2011). The higher $^{206}Pb/^{207}Pb$ ratios of the Boleo manganese mineralization

suggest diagenetic alteration by sedimentary pore waters due to the interaction with Th-rich fluids (Conly *et al.*, 2011). However, the new lead isotope data of the Boleo manganese oxides from the different mineralized mantos overlap the isotope fields for the ASL and the Boleo Formation rocks, suggesting similarities in the lead isotope ratios, and therefore an alternative explanation is that the metals involved in the manganese oxide mineralization in the Boleo mantos were leached from the ASL and Boleo Formation rocks (Figures 5a and 5b). The lead isotope field for the Boleo manto sulfides partially overlaps those of the Boleo manganese oxides, the ALS, and the Boleo Formation rocks, which suggests a source with similar isotopic composition for the metals. The isotopic shift can be explained by modifications in the isotope signature due to interactions with post-depositional fluids, which can be easily explained by the fine-grained nature (<50 μm) of the sulfide mineralization (Conly *et al.*, 2006).

Figure 6 shows the strontium and lead isotope compositions of the lithologic units and manganese oxides. In general the $^{87}Sr/^{86}Sr$ and $^{206}Pb/^{204}Pb$ isotope ratios for the ASL rocks and the Peninsular Ranges batholith have a constrained range and form a restricted field, as oppose to the rift-related rocks, which are characterized by lower $^{87}Sr/^{86}Sr$ ratios and less radiogenic lead. The most elevated $^{87}Sr/^{86}Sr$ ratios belong to the gypsum member of the Boleo Formation, which clearly has an important component of seawater as indicated by the Sr isotope composition of seawater at the time of deposition around 7 Ma (Figure 6) (McArthur *et al.*, 2001; Conly *et al.* 2011).

The manganese oxide mineralization from the Boleo district and surrounding areas is clearly located on a mixing trend between the high $^{87}Sr/^{86}Sr$ gypsum end-member and the low $^{87}Sr/^{86}Sr$ ASL and Peninsular Ranges batholith end-member (Figure 6). The elevated $^{87}Sr/^{86}Sr$ ratios in the manganese oxides from Boleo district indicate the incorporation of more radiogenic strontium in the mineralizing fluids, and could suggests an important involvement of seawater fluids during the formation of the mantos. The most probable explanation for the $^{87}Sr/^{86}Sr$ ratios is the interaction of the ascending fluids with the gypsum member located stratigraphically below the clastic sequence that hosts the mineralized mantos (Figure 2). The isotope field for the manganese oxides from Lucifer deposit is closer to the more radiogenic members of the ASL rocks and Peninsular Ranges batholith, suggesting that the involvement of seawater fluids during the mineralization processes was minimal.

The manganese oxides from the Gavilán deposit in Concepción Peninsula show $^{87}Sr/^{86}Sr$ similar to those from Lucifer deposit and a $^{206}Pb/^{204}Pb$ isotope ratio within the range of ASL rocks (Conly, 2003; Conly *et al.* 2005, 2006, and 2011) and the more radiogenic end-member of the rift-related rocks (Conly, 2003; Conly *et al.* 2005, 2006, and 2011) (Figure 6). The Sr isotope signature of the ASL rocks in Concepción Peninsula is similar to that of the manganese oxide from Lucifer deposit; therefore, a minimal

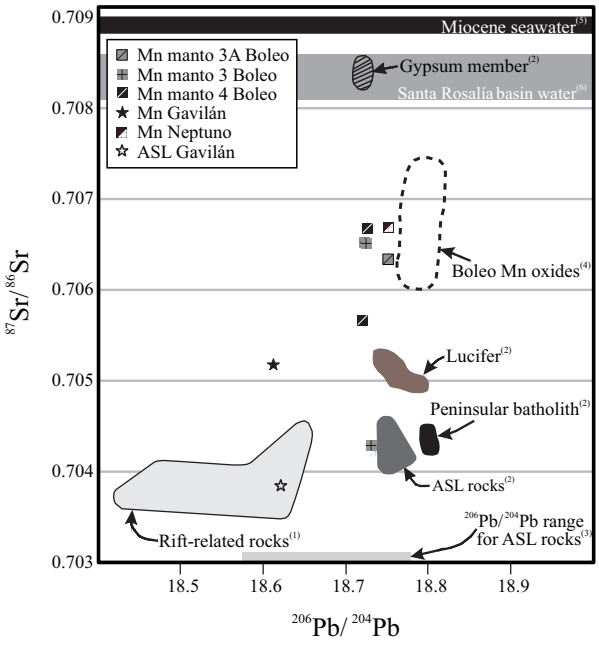

Figure 6. $^{206}Pb/^{204}Pb$ *vs.* $^{87}Sr/^{86}Sr$ diagram for the manganese oxide mineralization from the Boleo district and nearby areas. Rock fields taken from (1) Conly (2003); (2) Del Rio Salas (2011); (3) Conly *et al.* 2005, 2006, 2011; (4) Conly *et al.* (2011); (5) McArthur *et al.* (2001).

interaction with seawater is interpreted for the manganese oxide mineralizing fluids. The lead and strontium isotope signatures of the manganese oxides clearly shows that the rift-related volcanics are not the source of metals for the manganese mineralization, and that the ASL rocks undoubtedly act as the most important source, with a minor role of the Peninsular Ranges batholith rocks.

Manganese oxide mineralization and regional implication

The constraints on the genesis of the manganese oxides along the eastern coast of Baja California contributes to the understanding of metallogenetic processes during the proto-rift to rifting tectonics of the Gulf of Baja California. Hydrothermal activity and manganese oxide mineralization is recorded along a stretch of 200 km on the eastern coast from Lucifer deposit, located in the northwestern portion, to the Cerro Mencenares volcanic field, located in the southeastern portion (Figure l).

The most reliable age for the manganese oxides from the Boleo district is obtained from a hydrothermal manganese oxide-quartz vein hosted in manto 4, constrained to 7 Ma, which is within the range of the Boleo Formation deposition age (Conly *et al.*, 2011). Lucifer deposit correlates with manto 4 of the Boleo district, and is considered to have been located within the margin zones of the basin when the Boleo Formation was deposited (Del Rio Salas *et al.*, 2008). Therefore, on the basis of geological correlation

and fieldwork observations, a similar manganese oxide age (~7 Ma) is interpreted for the Lucifer deposit. This age is also consistent with the geochronological constraints for the 24–13 Ma volcanic rocks of Andesita of Sierra Santa Lucía (Sawlan and Smith, 1984; Conly *et al.*, 2005) that is hosting manganese oxide veins underlying the Lucifer deposit.

In contrast, the southern manganese mineralization, such as those in Santa Rosa and Juanico, is constrained to Pliocene structures (González-Reyna, 1956; Terán-Ortega and Ávalos-Zermeño, 1993; Umhoefer *et al.*, 2002), therefore, the hydrothermal activity responsible for the manganese mineralization in this area is younger than the geochronologic data reported for the Boleo district by Conly *et al.* (2011). In addition to this, volcanic activity such as the Pliocene Mencenares volcanic center is reported to be coeval with the manganese mineralization (Bigioggero *et al.*, 1995), which suggests the migration of the mineralization activity to the south of the Boleo district, as evidenced also by the present day hydrothermal activity reported in Concepcion Bay by Prol-Ledesma *et al.* (2004).

The geology and the available geochronological data suggest a southward migration of the hydrothermal processes related to the evolving tectonic regime of the opening of the Gulf of California. In detail, such southward migration is recorded at a smaller scale within the Santa Rosalía basin, where the southward migration, due to the basin subsidence, is recorded by the presence of the first two sedimentary cycles (4 and 3) in the north sub-basin, whereas the last sedimentary cycles (2 to 0) are present in both north and south sub-basins (Conly *et al.*, 2006). The migration of the hydrothermal activity can be explained as a response of the regional southward trend of Proto-Gulf extension (Stock and Hodges, 1989).

The lead isotope systematics support the southward migration by the isotopic trend from a more radiogenic end-member to a less radiogenic end-member that geographically correspond to the Peninsular Ranges batholith located in northwestern portion, and to Concepción Peninsula in the southeastern portion, respectively (Figure 5b). The available lead isotope data suggests a migration of the hydrothermal processes where: 1) the metals were leached mostly from ASL rocks with minor involvement Peninsular Ranges batholith in the southern manganese oxide localities, and 2) the thermal energy was supplied by magmatism, or by the increase of geothermal gradient related to crustal thinning, or a combination of both, related to the evolving context of the opening of the Gulf of California. More lead isotope data are needed to support the proposed migration, especially in younger manganese oxide localities of the southeastern areas (*i.e.* Santa Rosa and Juanico).

CONCLUSIONS

The geological context, the hydrothermal activity, and the Mn mineralization in the Boleo district, in conjunction with the manganese deposits of the eastern coast of Baja California, confirm the strong relationship between metallogenetic processes and the evolution of the proto-rift to rifting tectonics of the Gulf of Baja California

The trace element concentrations in the manganese oxides from the Boleo mantos, in conjunction with those for the manganese mineralization from Lucifer, Neptuno, and the manganese deposits from Concepción Peninsula, demonstrate the hydrothermal origin and the exhalative nature for all manganese deposits reported in the present study. The REE geochemistry in the manganese oxides supports the hydrothermal nature and excludes the hydrogenous nature for the manganese oxides.

Lead isotopes demonstrate that the sources for the ore metals in the Santa Rosalía region are the ASL rocks and the Peninsular Ranges batholith. In contrast, the early-rift volcanic rocks, which are nearly coeval with the mineralization, do not contribute with metals for the ore-forming processes, although they could have contributed with thermal energy to promote the hydrothermal activity. The lead isotope systematics also support a southward migration of the hydrothermal processes, indicated by the isotopic trend from a more radiogenic end-member to a less radiogenic end-member, from Lucifer deposit located at the northwest, to Concepción Peninsula in the southeastern portion. Field observations and Pb and Sr isotope signatures show that the fluids involved in the Mn mineralization from the Boleo district are essentially hydrothermal and exhalative in origin; the isotope signatures show that mineralizing fluids interacted with two end-members: 1) ASL rocks and the Peninsular Ranges batholith, and 2) the gypsum member of the Boleo Formation. The isotope data supports a less radiogenic nature for the fluids involved in the genesis of the manganese oxides from Lucifer in the Boleo area and Gavilán in the Concepción Peninsula, suggesting less involvement of seawater fluids.

ACKNOWLEDGMENTS

This research was supported by the Consejo Nacional de Ciencia y Tecnología (CONACYT) grant 166600. We are thankful to Francisco Escandón for the earlier support and helpful discussions. We are also thankful to Baja Mining Corp by the logistical and fieldwork assistance, especially to Tawn Albinson, Roberto Gastélum, Elisiel Moreno, and Lorenzo Ruiz. Finally, we would like to thank Andrew Conly, Nursel Oksuz, and Carles Canet for their revisions and constructive comments.

REFERENCES

Atwater, T., 1989, Plate tectonic history, northeastern Pacific and western North America, *in* Winterer E.L., Hussong D.M., Decker R.W. (eds.), The eastern Pacific Ocean and Hawaii: Geological Society of America, The Geology of North America, v. N, 21-72.

Bailes, R.J., Christoffersen, J.E., Escandon, V.F., Peatfield, G.R., 2001, Sediment-hosted deposits of the Boléo copper-cobalt-zinc district, Baja California Sur, Mexico, *in* Albinson, T., Nelson, C.E. (eds), New mines and discoveries in Mexico and Central America: Society of Economic Geologist, Special Publication 8, 291-306.

Bigioggero, B., Chiesa, S., Zanchi, A., Montrasio, A., Vezzoli, L., 1995, The Cerro Mencenares volcanic center, Baja California Sur: Source and tectonic control on postsubduction magmatism within the Gulf Rift: Geological Society of America Bulletin, 107, 1108-1122.

Bonatti, E., Kraemer, T., Rydell, H., 1972, Classification and genesis of submarine iron-manganese deposits, *in* Horn, D. (ed.), Ferromanganese deposits on the ocean floor: Washington, D. C., National Science Foundation, 149-166.

Bustamante García, J., 1999, Monografía Geológico-Minera del Estado de Baja California Sur: México, Secretaría de Comercio y Fomento Industrial, Coordinación General de Minería, 180 pp.

Camprubí, A., Canet, C., Rodríguez-Díaz, A., Prol-Ledesma, R, Blanco-Florido, D., Villanueva, R., López-Sánchez, A., 2008, Geology, ore deposits and hydrothermal venting in Bahía Concepción, Baja California Sur, Mexico: Island Arc, 17, 6-25.

Canet, C., Prol-Ledesma, R.M., Proenza, J., Rubio-Ramos, M.A., Forrest, M.J., Torres-Vera, M.A., Rodríguez-Díaz, A., 2005, Mn-Ba-Hg mineralization at shallow submarine hydrothermal vents in Bahía Concepción, Baja California Sur, Mexico: Chemical Geology 224, 96-112.

Canet, C., Prol-Ledesma, R.M., Bandy, W.L., Schaaf, P., Linares, C., Camprubí, A., Tauler, E., Mortera-Gutiérrez, C., 2008, Mineralogical and geochemical constraints on the origin of ferromanganese crusts from the Rivera Plate (western margin of Mexico): Marine Geology, 251, 47-59.

Casarrubias, U.Z., Gómez-López, G., 1994, Geología y evaluación geotérmica de la zona de Bahía Concepción, Baja California Sur, México, *in* Resúmenes de la 3a Reunión Internacional sobre geología de la Península de Baja California: La Paz Baja California Sur, México, Universidad Autónoma de Baja California Sur, 22-23.

Chesley, J., Ruiz, J., Righter, K., Ferrari, L., Gómez-Tuena, A., 2002. Source contamination versus assimilation: an example from the Trans-Mexican volcanic arc: Earth and Planet Science Letters, 195, 211-221.

Conly, A.G., 2003, Origin of the Boleo Cu-Co-Zn deposit, Baja California Sur, México: Implications for the interaction of magmatic-hydrothermal fluids in a low-temperature hydrothermal system: Toronto, Canada, University of Toronto, Ph.D. Thesis, 433 pp.

Conly, A.G., Brenan, J.M., Bellon, H., Scott, S.D., 2005, Arc to rift transitional volcanism in the Santa Rosalía region, Baja California Sur, México: Journal of Volcanology and Geothermal Research, 142, 303-341.

Conly, A.G., Beaudoin, G., Scott, S.D., 2006, Isotopic constraints on fluid evolution and precipitation mechanisms for the Boléo Cu–Co–Zn district, Mexico: Mineralium Deposita, 41(2), 127-151.

Conly, A.G., Scott, S.D., Bellon, H., 2011, Metalliferous manganese oxide mineralization associated with the Boleo Cu-Co-Zn district, Mexico: Economic Geology, 106, 1173-1196

Crerar, D.A., Namson, J., Chyi, M.S., Williams, L., Feigenson, M.D., 1982, Manganiferous cherts of the Franciscan assemblage: I. General geology, ancient and modern analogues, and implications for the hydrothermal convection at oceanic spreading centers: Economic Geology, 77, 519-540.

Del Rio Salas, R., Ruiz J., Ochoa Landín, L., Noriega, O., Barra, F., Meza-Figueroa, D., Paz Moreno, F., 2008, Geology, Geochemistry and Re–Os systematics of manganese deposits from the Santa Rosalía Basin and adjacent areas in Baja California Sur, México: Mineralium Deposita, 43, 467-482.

Del Rio Salas, R., 2011, Metallogenesis for the Boléo and Cananea Copper Mining Districts: a contribution to the understanding of copper ore deposits in Northwestern Mexico: Tucson, Arizona, University of Arizona, Ph.D. dissertation, 259 pp.

Douville, E., Bienvenu, P., Charlou, J.L., Donval, J.P., Fouquet, Y., Appriou, P., Gamo, T., 1999, Yttrium and rare earth elements in fluids from various deep-sea hydrothermal systems: Geochimica et Cosmochimica Acta, 63, 627-643.

Elderfield, H., Greaves, M.J., 1981, Negative cerium anomalies in the rare earth element patterns of oceanic ferromanganese nodules: Earth and Planetary Science Letters, 55, 163-170.

Fleet, A.J., 1983, Hydrothermal and hydrogenous ferromanganese deposits: Do they form a continuum? The rare earth element evidence, *in* Rona, P.A., Boström, K., Laubier, L., Smith, K.L. (eds), Hydrothermal Process at Seafloor Spreading Centers: New York, Plenum Press, 535-555.

Freiberg, D.A., 1983, Geologic setting and origin of the Lucifer manganese deposit, Baja California Sur, México: Economic Geology, 78, 931-43.

Gastil, G., Phillips, R., Allison, E., 1975, Recconaissance geology of the State of Baja California: The Geologial Society of America, Memoir 140, 169 pp.

Glasby, G.P., Stüben, D., Jeschke, G., Stoffers, P., Garbe-Schönberg, C.D., 1997, A model for the formation of hydrothermal manganese crusts from the Pitcairn Island hotspot: Geochimica et Cosmochimica Acta, 61, 4583-4597.

González-Reyna, J., 1956, Los yacimientos de manganeso de El Gavilán, La Azteca y Guadalupe, Baja California, México, *in* González-Reyna, J. (ed.), Symposium sobre yacimientos de manganeso, v. III: XX Congreso Geológico Internacional, Mexico City, 79-96

Gromet, L.P., Dymek, R.F., Haskin, L.A., Korotev, R.L., 1984, The "North American Shale Composite": its implication, major and trace element characteristics: Geochimica et Cosmochimica Acta, 48, 2469-2482.

Hausback, B.P., 1984, Cenozoic volcanism and tectonic evolution of Baja California Sur, Mexico, *in* Frizzel, Virgil A. Jr, (ed.), Geology of the Baja California Peninsula: Pacific Section S.E.P.M., 39, 219-236.

Hodkinson, R.A., Stoffers, P., Scholten, J., Cronan, D.S., Jeschke, G., Rogers, T.D.S., 1994, Geochemistry of hydrothermal manganese deposits from the Pitcairn Island hotspot, southeastern Pacific: Geochimica et Cosmochimica Acta, 58, 5011-5029.

Holt, J.W., Holt, E.W., Stock, J.M., 2000, An age constraint on Gulf of California rifting from Santa Rosalia basin, Baja California Sur, Mexico: Geological Society of America Bulletin 112, 540-549.

Karig, D.E., Jensky, W., 1972, The protogulf of California: Earth and Planetary Science Letters, 17, 169-172.

Lonsdale, P., 1989, Geology of tectonic history of the Gulf of California, *in* Winterer, E.L., Hussong D.M., Decker R.W. (eds.), The Eastern Pacific Ocean and Hawaii: Geological Society of America, The Geology of the North America, v. N, 499-522.

McArthur, J.M., Howarth, R.J., Bailey, T.R., 2001, Strontium isotope stratigraphy: LOWESS version 3: best fit to the marine Sr-isotope curve for 0-509 Ma and accompanying look-up table for deriving numerical age: The Journal of Geology, 109, 155-170.

Michard, A., Albarède, F., Michard, G., Minster, J.F., Charlou, J.L., 1983, Rare-earth elements and uranium in high-temperature solutions from the East Pacific Rise hydrothermal vent field (13ºN): Nature, 303, 795-797.

Miura, H., Hariya, Y., 1997, Recent manganese oxide deposits in Hokkaido, Japan, *in* Nicholson, K., Hein, J.R., Bühn, B., Dasgupta, S. (eds), Manganese mineralization: geochemistry and mineralogy of terrestrial and marine deposits: The Geological Society London, Special Publication 119, 281-299.

Nath, B.N., Balaram, V., Sudhakar, M., Plüger, W.L., 1992, Rare earth element geochemistry of ferromanganese deposits from the Indian Ocean: Marine Chemistry, 38, 185-208.

Nath, B.N., Plüger, W.L., Roelandts, I., 1997, Geochemical constraints on the hydrothermal origin of ferromanganese encrustations from the Rodriguez Triple Junction, Indian Ocean, *in* Nicholson. K., Hein J.R., Bühn, B., Dasgupta, S. (eds), Manganese mineralization: geochemistry and mineralogy of terrestrial and marine deposits: The Geological Society London, Special Publication 119, 199-211 .

Nicholson, K., 1992, Contrasting mineralogical-geochemical signatures of manganese oxides; guides to metallogenesis: Economic Geology

87, 1253-1264.

Noble, J.A., 1950, Manganese on Punta Concepción, Baja California, Mexico: Economic Geology, 45, 771-785.

Ochoa-Landín, L., 1998, Geological, sedimentological and geochemical studies of the Boléo Cu-Co-Zn deposit, Santa Rosalía, Baja California, Mexico: Tucson, Arizona, University of Arizona, Ph.D. Thesis, 148 pp.

Ochoa-Landín, L., Ruiz, J., Calmus, T., Pérez, E., Escandon, F., 2000, Sedimentology and stratigraphy of the Upper Miocene Boleo Formation, Santa Rosalía, Baja California, Mexico: Revista Mexicana de Ciencias Geológicas, 17, 83-95.

Ortlieb, L., Colletta, B., 1984, Síntesis cronoestratigráfica sobre el Neogeno y el Cuaternario marino de la cuenca de Santa Rosalía, Baja California Sur, México, *in* Malpica-Cruz, V., Celis-Gutiérrez, S., Guerrero-García, J., Ortlieb, L. (eds.), Neotectonics and Sea Level Variations in the Gulf of California Area, a Symposium, Abstracts: México, D.F., Universidad Nacional Autónoma de México, Instituto de Geología, 242-268.

Pallares, C., Bellon, H., Benoit, M., Maury, R.C., Aguillón-Robles, A., Calmus, T., Cotten, J., 2008, Temporal geochemical evolution of Neogene volcanism in northern Baja California (27°–30° N): Insights on the origin of post-subduction magnesian andesites: Lithos, 105, 162-180.

Parr, J.M., 1992, Rare-earth element distribution in the exhalites associated with Broken Hill-type mineralisation at the Pinnacles deposit, New South Wales, Australia: Chemical Geology, 100, 73-91.

Portugal, E., Birkle, P., Barragan, R.R.M., Arellano, G.V.M., Tello, E., Tello, M., 2000, Hydrochemical-isotopic and hydrogeological conceptual model of the Las Tres Vírgenes geothermal field, Baja California Sur, Mexico: Journal of Volcanology and Geothermal Research, 101, 223-244.

Prol-Ledesma, R.M., Canet, C., Torres-Vera, M.A., Forrest, M.J., Armienta, M.A., 2004, Vent fluid chemistry in Bahía Concepción coastal submarine hydrothermal system, Baja California Sur, México: Journal of Volcanology and Geothermal Research, 137, 311-328.

Rodríguez-Díaz, A.A., Blanco-Florido, D., Canet, C., Gervilla-Linares, F., González-Partida, E., Prol-Ledesma, R.M., Morales-Ruano, S., García-Valles, M., 2010, Metalogenia del depósito de manganeso Santa Rosa, Baja California Sur, México: Boletín de la Sociedad Geológica Mexicana, 62, 141-159

Roy, S., 1992, Environments and processes of manganese deposition: Economic Geology, 87, 1218-1236

Sawlan, M.G., Smith, J.G., 1984, Petrologic characteristics, age and tectonic setting of Neogene volcanic rocks in Northern Baja California Sur, Mexico, *in* Frizzel, V.A. (ed.), Geology of the Baja California Peninsula: Pacific Section S.E.P.M., 39, 237-251.

Sawlan, M.G., 1991, Magmatic evolution of the Gulf of California Rift, *in* Dauphin, J.P., Simoneit, B.R.T. (eds.), The Gulf and Peninsular Province of the Californias: American Association of Petroleum Geologists, 47, 301-369.

Schmidt, E.K., 1975, Plate tectonics, volcanic petrology, and ore formation in the Santa Rosalía area, Baja California, Mexico: Tucson AZ, University of Arizona, M. Sc. thesis, 194 pp.

Schmitt, A.K., Stockli, D.F., Niedermann, S., Lovera, O.M., Hausback, B.P., 2010, Eruption ages of Las Tres Vírgenes volcano (Baja California): A tale of two helium isotopes: Quaternary Geochronology, 5, 503-511.

Spencer, J.E., Normark, W.R., 1989, Neogene plate-tectonic evolution of the Baja California Sur continental margin and the southern Gulf of California, *in* Winterer, E.L., Hussong, D.M., Decker, R.W. (eds), The Eastern Pacific Ocean and Hawaii: Geological Society of America, The Geology of the North America, v. N, 489-498.

Stock, J.M., Hodges, K.V. 1989, Pre-Pliocene extension around the Gulf of California and the transfer of Baja California to the Pacific Plate: Tectonics, 8, 99-115.

Terán-Ortega, L.A., Ávalos-Zermeño, A., 1993, Prospecto Las Mantitas, área Bahía Concepción, Municipio de Mulegé, Baja California Sur: México D.F., Consejo de Recursos Minerales, Reporte Técnico, 65 pp.

Thibodeau, A.M., Killick, D.J., Ruiz, J., Chesley, J.T., Deagan, K., Cruxent, J.M., Lyman, W., 2007, The strange case of the earliest silver extraction by European colonists in the New World: Proceedings of the National Academy of Sciences, 104, 3663-3666.

Umhoefer, P.J., Dorsey, R.J., Willsey S., Mayer, L., Renne P., 2001, Stratigraphy and geochronology of the Comondú Group near Loreto, Baja California Sur, Mexico: Sedimentary Geology, 144, 125-47.

Umhoefer, P.J., Mayer, L., Dorsey, R.J., 2002, Evolution of the margin of the Gulf of California near Loreto, Baja California Peninsula, Mexico: Geological Society of America Bulletin, 114, 849-868.

Usui, A., Someya, M., 1997, Distribution and composition of marine hydrogenetic and hydrothermal manganese deposits in the northwest Pacific, *in* Nicholson, K., Hein, J.R., Bühn, B., Dasgupta, S. (eds), Manganese Mineralization: Geochemistry and mineralogy of terrestrial and marine deposits: The Geological Society London, Special Publication 119, 177-198.

Wilson, I.F., Veytia, M., 1949, Geology and manganese deposits of the Lucifer district northwest of Santa Rosalía, Baja California, Mexico: Wasshington D.C., United States Department of the Interior, Geological Survey, Bulletin 960-F, 177-231.

Wilson, I.F., Rocha, V.S., 1955, Geology and Mineral Deposits of the Boleo Copper District Baja California, Mexico: United States Geological Survey, Professional Paper 273, 134 pp.

Wiltshire, J.C., Wen, X.Y., Yao, D., 1999, Ferromanganese crusts near Johnston Island: Geochemistry, stratigraphy and economic potential: Marine Georesources and Geotechnology, 17, 257-27.

Zheng, Y.F., 1991, Calculation of oxygen isotope fractionation in metal oxides: Geochimica et Cosmochimica Acta, 55, 2299-2307.

Manuscript received: August 15, 2013
Corrected manuscript received: October 18, 2013
Manuscript accepted: October 22, 2013